博士論文

Hierarchical visual form processing of Japanese *Kanji* characters in the ventral visual pathway

（腹側視覚路における日本語漢字の階層的視覚形態認知）

平成 28 年度

筑波大学大学院　人間総合科学研究科　感性認知脳科学専攻

樋口　大樹

Contents

Chapter I Introduction 1

1. Cognitive processing of Chinese and Japanese *Kanji* characters 1

2. Neural substrates of reading: Clues from neuropsychological studies 7

3. Neural abnormalities in individuals with developmental dyslexia 14

4. Visual word and character form processing in the brain 19

Chapter II Purpose 25

Chapter III Experiment 1: Visual form processing of Japanese *Kanji* character 27

1. Purpose 27

2. Materials and Methods 27

2.1. Participants 27

2.2. Stimuli 28

2.3. Experimental Design 29

2.4. fMRI data acquisition and analysis 31

3. Results 35

3.1. Behavioral data of the size judgment task 35

3.2. fMRI data 38

4. Discussion 47

Chapter IV Experiment 2: Visual processing of objects 53

1. Purpose 53

2. Materials and Methods 53

2.1. Participants 53
2.2. Stimuli 54
2.3. Experimental Design 56
2.4. fMRI data acquisition and analysis 57
3. Results 60
3.1. Behavioral data of the size judgment task 60
3.2. fMRI data 63
4. Discussion 72
Chapter V General discussion 75
References 81
Appendix A 92
Appendix B 95

Chapter I Introduction

1. Cognitive processing of Chinese and Japanese *Kanji* characters

How are the visual forms of Japanese *Kanji* characters recognized? There are a limited number of studies on Japanese *Kanji* characters. However, a series of studies has been carried out regarding Chinese characters. It has been a long-standing question whether Chinese characters are processed holistically or hierarchically. Most of the Chinese characters consist of submorphemes, similar to Japanese *Kanji* characters. These include “朴”, which can be separated into a left component, “木”, and a right component, “卜”. Furthermore, each submorpheme consists of a combination of strokes. It is natural to think that Chinese single characters are recognized in a hierarchical manner. Cognitive psychologists have examined this idea empirically. Studies of physical features of Chinese characters support holistic processing. Stroke number does not influence performance on lexical decision tasks, where participants are required to judge whether the presented Chinese character is real or not (Chen & Yung, 1989). This stroke effect was not replicated in other studies evaluating performance in character naming and lexical decision tasks (Leong, Cheng, & Mulcahy, 1987; Tan, Hoosain, & Peng, 1995). These studies imply that stroke and/or related visual features are processed before processing of the whole character. In research on cognitive processing of radicals, scientists have tried to describe cognitive processing of radicals using behavioral measurements. The first paradigm is the illusory conjunction, where two or more stimuli exposed very close to each other in time tend to be miss-recognized such that the components of the stimuli are recombined (Allport, 1977; Shallice & McGill, 1978).

For instance, when a green circle and a red triangle are presented at the same time, participants might report that only a green triangle is presented. Radical processing of Chinese characters was assessed using this phenomenon. Two Chinese characters (e.g., “他” and “淋”) are presented very briefly followed by Chinese characters that are combinations of the presented stimuli (e.g., “休”). Participants are required to judge whether the presented stimulus (“休”) is the same as the previously presented stimuli. A “yes” response may be considered an index of illusory conjunction. Some studies of Chinese characters have indicated the presence of this illusory conjunction (Fang & Wu, 1989; Lai & Huang, 1988). This implies that Chinese radicals play a critical role in Chinese character processing. The naming task is another tool used to investigate the roles of Chinese radicals. A significant effect of radical frequency was observed in the character naming task, such that high frequency radicals produced faster naming times (Han, 1994). Similar results were found by another research group (Peng, Li, & Yang, 1997). This shows the importance of radical representation for Chinese character recognition, which is demonstrated by the illusory conjunction effect. The third tool used to investigate Chinese radical processing is the lexical decision task, where participants are required to indicate whether the presented stimuli are real characters. In this task, radical frequency significantly affects lexical decision time (Taft & Zhu, 1997). Based on this and the previous studies, the authors proposed a multilevel interactive-activation framework for the processing of Chinese words (Figure 1). The interactive activation framework for reading was originally proposed for non-logographic scripts, which are made up of different levels of units, such as words, letters, and features (McClelland & Rumelhart, 1981; Rumelhart & McClelland, 1982).

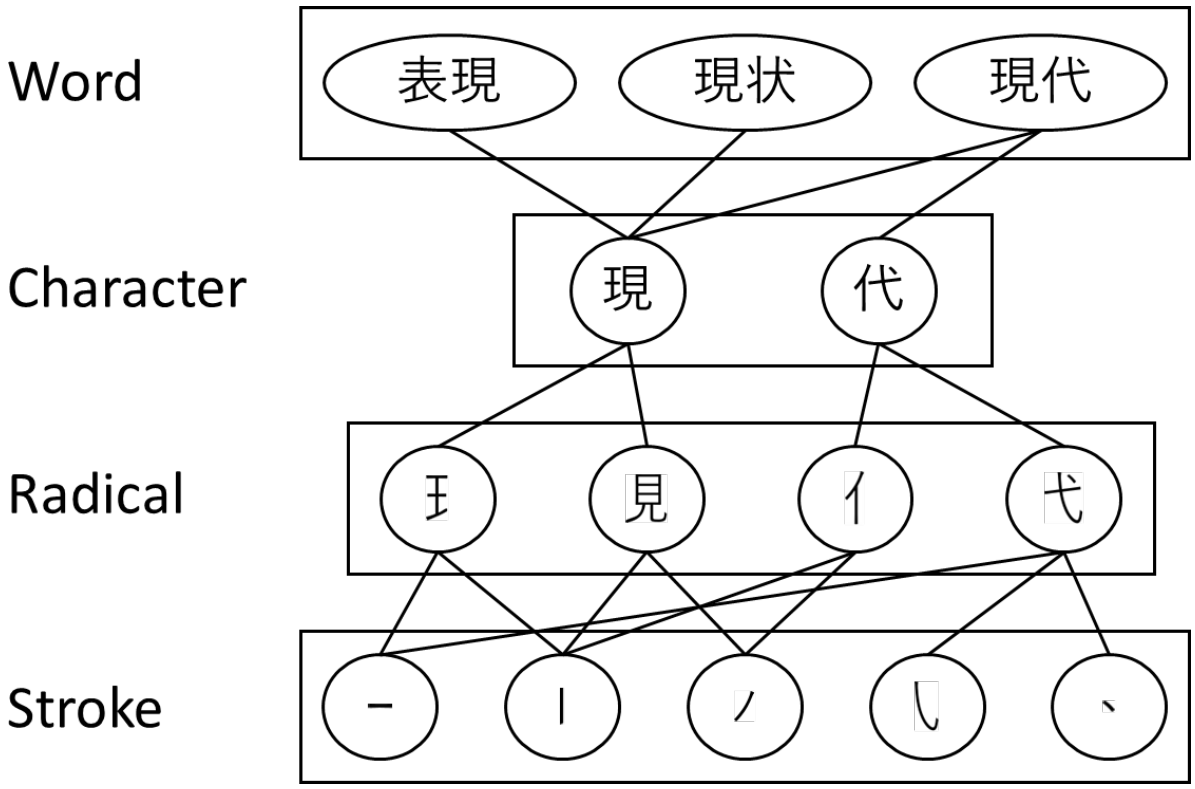

Figure 1 A multilevel interactive-activation framework for the processing of Chinese words, proposed by Taft and Zhu (1997).

The interactive-activation framework in Chinese words was created by adapting such an interactive model, such that the Chinese model consists of multiple levels of lexicon components, such as strokes, radicals, and characters. Each component is interactively connected to the others. Upon comparing the interactive-activation model for Chinese and non-logographic scripts, a Chinese character involves hierarchical processing (i.e., radicals and strokes), while letters of an alphabet are just coding combinations of local features. Nowadays, more sophisticated reading models are proposed for alphabetic scripts (Coltheart, Rastle, Perry, Langdon, & Ziegler, 2001; Perry, Ziegler, & Zorzi, 2007), but the lexicon for sub-words has not been modeled. Thus, the presence of hierarchical components for characters seems to be a characteristic of logographic scripts. The interactive-activation framework for reading Chinese has been used as a theoretical framework in recent studies(Su, Mak, Cheung, & Law, 2012; Zhou, Peng, Zheng, Su, & Wang, 2012) and is supported by other research (Taft et al., 1999). For example, characters consisting of high transposable radicals did not produce longer response times and were judged to be real Chinese characters when compared to characters consisting of low transposable radicals. When I consider vertically structured characters such as “呆”, I can calculate how often upper radicals (“口”) are used in the upper position vs. the lower position. Radicals that tend to be used in inconsistent positions are referred to as being high-frequency transposable radicals. In this case, both the upper and lower radicals are highly transposable, as both radicals tend to be used in both positions (i.e., “呆” and “杏”). When the character “呆” is presented, position-free radical representations could easily lead to confusion between “呆” and “杏” and result in longer response times. A more recent study validated the hierarchical representation

of Chinese characters using priming experiments (Ding, Peng, & Taft, 2004). They found significant facilitation effects of radicals for low frequency target characters. Specifically, facilitation was observed in target-shared radicals at the same position, but not at different positions, during the lexical decision task. This result supports the position-specific representation of Chinese characters, which was reported in a previous study (Taft et al., 1999). Most studies aimed at uncovering the cognitive processes underlying logographic character recognition have been carried out for Chinese characters. However, there are limited numbers of studies examining the cognitive process underlying the recognition of logographic Japanese *Kanji* characters. Some of the radicals in Japanese *Kanji* characters represent phonological and semantic information, as in Chinese characters. For instance, the Japanese *Kanji* character “校” consists of a left side radical, “木”, and a right side radical, “交”. The left side radical, which means tree in this case, is sometimes called a semantic radical while the right side radical is called a phonetic radical. The pronunciation of the whole character, /kou/, derives from the pronunciation of the phonetic radical. In Japanese *Kanji* characters, the early exposure of phonetic radicals produce a facilitation effect in the naming task (Flores d’Arcais, Saito, & Kawakami, 1995). Another study replicated this phonetic facilitation effect and found the consistency effects of radicals (Saito, Masuda, & Kawakami, 1999). The consistency effect of a radical depends on the number of pronunciations of a phonetic radical in the character. For example, the phonetic radical “帝” is a consistent radical and has only one pronunciation in characters such as “諦” and “蹄”. However, “寺” is an inconsistent radical and may be pronounced as “侍” (/ji/), “特” (/toku/), or “詩” (/si/). If phonological information of the phonetic radical is used

when I read *Kanji* characters, characters including consistent radicals should be read faster than those with inconsistent radicals. Inconsistent radicals have multiple candidate pronunciations that may lead to competition in the radical lexicon. In contrast, the consistent radicals activate a limited number of nodes. As a result, information by radical lexicons is conveyed faster than information by inconsistent radicals. Thus, the consistency effect of a radical can be explained using a multilevel interactive-activation framework. In summary, cognitive psychological studies have shown that Chinese and Japanese *Kanji* characters are processed by hierarchical manner.

2. Neural substrates of reading: Clues from neuropsychological studies

In 1891 and 1892, Dejerine described two historical cases. The first patient suffered from alexia with agraphia and had impairments in both reading and writing. The patient had a lesion in the left angular gyrus, but the other language areas, such as Wernicke's and Broca's areas, were intact. Based on this case, Dejerine concluded that visual representations of letters are stored in the left angular gyrus. This is because the lesion in the angular gyrus impaired the decoding and encoding of visual representations of letters and resulted in impairments in reading and writing. The second patient presented with an acute loss of the ability to read letters and words. The central part of the damage was localized to the white matter tract of the lingual gyrus. There was also a lesion in the corpus callosum. Dejerine interpreted the pathology of the second case as follows. Since the patient's visual representation of letters was preserved, the left angular gyrus must have been intact in this patient. Visual information need to reach the left angular gyrus for us to be able to read words. However, lesions in the left lingual gyrus disrupt the conveyance of visual information from this region to the left angular gyrus. Unfortunately, this "disconnection" theory was long neglected, at least in the United States and the United Kingdom, until Geschwind renewed interest in the theory. In 1965, Geschwind published his landmark review article "Disconnexion syndromes in human and man" in Brain, where he reevaluated the disconnection theory proposed by Dejerine. One of the criticisms of Dejerine's theory is that the theory cannot explain intact object-naming ability in patients with selective reading impairments. According to Dejerine's model, connection to the left angular gyrus is mandatory in object naming, as he believed that the angular gyrus is the gateway to

language production. Geschwind tried to renew the disconnection model proposed by Dejerine as follows. Flechsing's principle states that the primary sensory cortex is connected only to near "association areas", which are the lately myelinated brain regions proposed by Flechsing (Flechsig, 1901). The part of the visual cortex surrounded by the primary visual cortex is referred to as the "visual association cortex". Additionally, animal experiments by Flechsings and others indicate that the primary visual area has no callosal connection. Based on these observations, Geschwind (1965) tried to rebuild the disconnection model of reading and writing. He hypothesized three potential pathways for language processing and attempted to find the model that could explain previously reported cases (Figure 2). The first possible pathway goes through the right area 17, right visual association cortex, right angular gyrus, and finally crosses the corpus callosum and reaches the left angular gyrus. The second possible pathway runs from the right area 17 to the right visual association cortex and then crosses the corpus callosum and finally reaches the left angular gyrus through the left visual association cortex. The third possible pathway is that both pathways are used. Preserved object-naming ability in patients with acquired reading impairments can be explained by the first possibility. Objects may have rich associations with other modalities (e.g., smell, taste, and touch). This may result in information processing in higher brain areas. The information may then pass across the anterior part of the corpus callosum to the left angular gyrus. In Dejerine's patient, the posterior part of the corpus callosum was impaired, but the anterior corpus callosum was intact. This enabled the patient to name objects. The patient who had the left occipital lobe removed had reading impairments at first. However, his reading impairments were overcome. This

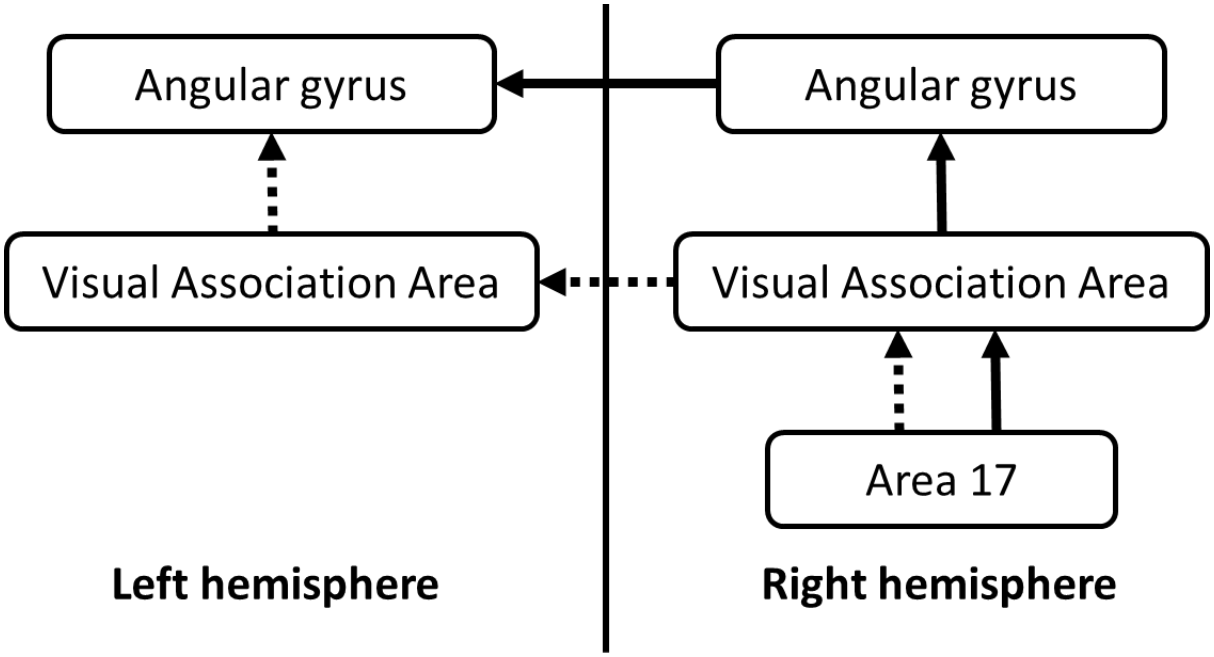

Figure 2 Tentative reading model proposed by Geschwind (1965). This figure shows a hypothesized brain network for reading and writing. Geschwind assumed the presence of three possible pathways. The first possible pathway illustrated in solid lines connects area 17 with the left angular gyrus via the right visual association cortex and the right angular gyrus. In the second possible pathway illustrated in dotted lines, information is conveyed to the right visual association area through the arcuate fasciculus and visual association area. The third possible pathway involves the use of both pathways.

pathway may be involved in reading in some way. However, it was ruled out as an exclusive pathway. Thus, the third possibility is supported. Dejerine speculated that the left angular gyrus stores the visual representations of letters (Dejerine, 1891). However, Geschwind (1965) presumed that the angular gyrus is involved in cross-modal associations. Indeed, his group showed impairments in color naming which required to match colors (visual) and names (auditory) in patients with angular gyrus lesions. The studies of Dejerine and Geschwind set a basic framework for the cognitive function of the angular gyrus in reading. Nevertheless, the cognitive function of the visual association cortex is not very well understood based on their studies. Studies of pure alexia in patients who have selective impairments in word reading give us clues in our search for the function of the higher visual cortex in reading. Dejereine's patient has sometimes been used as an example in early descriptions of alexia. However, this case is now regarded as a case with global alexia, which indicates a complete inability to read words and letters (Binder & Mohr, 1992). Other similar cases have been reported by other research groups (e.g.,, Warrington & Shallice, 1980; Arguin & Bub, 1993). Pure alexia is an acquired reading disability and leads to patients reading words in a "letter- by-letter" manner. The patients can name each letter but cannot read whole words. This may reflect a visual word-form deficit. However, I need to discuss another possibility before I make this conclusion. Some researchers believe that letter-by-letter reading in acquired dyslexia is an element of "Simultanagnosia" (Behrmann, Nelson, & Sekuler, 1998). Simulatanagnosia was first proposed by Wolpert, who used it to refer to the inability to recognize two or more objects at once (Wolpert, 1924). For instance, simultanagnosia may be implicated in impairments in recognizing some things (e.g.,

objects or scenes) in whole. Patients may not be able to recognize characters as a whole, but may be able to recognize each letter. This results in letter-by-letter reading. To rule out this possibility, Warrington and Shallice carefully investigated the cognitive profile of patients with letter-by-letter reading and showed that peripheral visual factors, selective attention, and visual short-term memory do not account for letter-by-letter reading (Warrington & Shallice, 1980). This result implies that patients with letter-by-letter reading have poor representations of "visual word forms," which is a term first coined by the authors. Based on these results, the authors proposed a new reading model. According to this model, information processed in the early visual area is sent to the visual word form system. This is followed by phonological and semantic processing (Figure 3). Which part of the brain is involved in visual word form processing? Lesion studies show that left occipito-temporal cortex damage induces pure alexia (Damasio & Damasio, 1983; Beversdorf, Stommel, Allen, Stevens, & Lessell, 1997; Binder & Mohr, 1992). This implies a key role for this region in visual word form processing. Based on these studies, Cohen et al. (2000) closely assessed the brain anatomies and brain functions of patients with alexia who had similar symptoms to those of Dejerine's original case. Two patients with posterior callosum lesions completely failed to read out words presented in the left visual field, but not in the right visual field. Words presented in the right visual field activated the left occipito-temporal cortex, as in control subjects. However, words presented in the left visual field did not lead to this activation. This result implies that the mid portion of left fusiform gyrus in occipito-temporal cortex is devoted to visual word form processing. The authors named this brain region the "Visual Word Form Area (VWFA)." The authors also described the

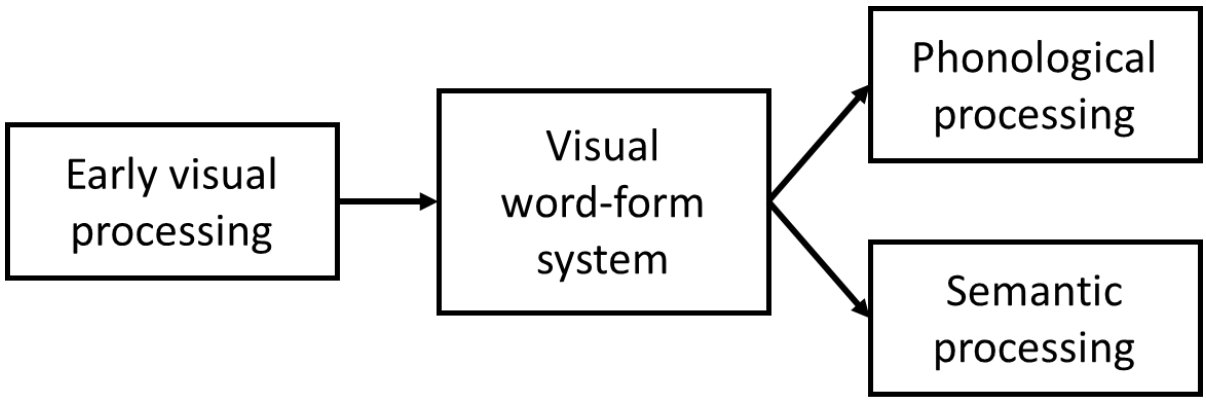

Figure 3 Reading model proposed by Warrington et al. (1980). The authors showed that letter-by-letter reading couldn't account for the impairment in early visual processing. Based on these findings, they proposed reading models where visually presented words are processed in the visual word form system. This is then followed by phonological and semantic processing.

functional and spatial properties of the VWFA (Cohen et al., 2002). Based on over 25 experiments, the peak coordinates of the VWFA are estimated to be x = −43, y = −54, z = −12 (Talairach coordinates) and brain activation in the VWFA is stronger for words than for consonants. This supports the presence of word form processing in this region. In summary, neuropsychological studies have enabled us to sketch a rough brain map for reading. In brief, visual word form information represented in the left occipito-temporal cortex is conveyed to the left inferior parietal lobule, which is devoted to phonological conversion, and is then processed semantically and phonologically.

3. Neural abnormalities in individuals with developmental dyslexia

Neuropsychological studies have contributed not only to our understanding of neural mechanisms of reading, but also to our understanding of the neural substrates of developmental dyslexia. Neuroimaging techniques enable us to investigate brain anatomy and function in people with developmental dyslexia. The first study of brain function in developmental dyslexia revealed hypoactivation of the left inferior parietal lobule during an auditory rhyme decision task (Rumsey et al., 1992). The second neuroimaging study measured brain activity during a visual rhyme judgement task, which replicated dysfunction in the left inferior temporal lobule in adult developmental dyslexia (Paulesu et al., 1996). In addition, other studies have also revealed hypoactivation in the left temporo-parietal region, including the inferior parietal lobule and posterior superior temporal gyrus, during phonological processing tasks in participants with developmental dyslexia (e.g., Shaywitz et al., 2002; Simos et al., 2000). Since converging evidence suggests that the core deficit in developmental dyslexia is phonological processing, the scopes of these neuroimaging studies involved the uncovering of brain responses in developmental dyslexia during phonological processing. Some subsequent studies investigated brain activity during reading. In a study in which participants performed explicit (reading) and implicit (judging whether the presented letters, such as b or f, are above midline) tasks, the left inferior and middle temporal regions were commonly activated by both tasks (Brunswick, McCrory, Price, Frith, & Frith, 1999). Additionally, the explicit task produced hyperactivation in the inferior frontal region in patients with developmental dyslexia, which may reflect a compensatory response. These results were replicated in another study the results of

which showed relative hypoactivation in the left temporo-parietal region, including Wernicke's area and angular gyrus, and hyperactivation in the inferior frontal gyrus (Shaywitz et al., 1998). Another study revealed abnormal brain magnetoencephalography (MEG) responses in the occipito-temporal cortex. People with developmental dyslexia did not show distinct word-specific activation at about 180 ms after word presentation in the left occipito-temporal area (Salmelin, Kiesilä, Uutela, Service, & Salonen, 1996). Previous studies have been performed using alphabetic scripts, such as those used in English, Italian, and French, even though these languages have completely different orthographic systems. For example, Italian letters tend to map onto one or small numbers of sounds (shallow orthography), while English letters tend to map onto multiple sounds (deep orthography). As a result, reading texts with shallow orthography is easier than reading texts with deep orthography. It is worth investigating whether people with developmental dyslexia have common biological bases affecting different orthographies. Paulesu et al. (2001) directly addressed this question by comparing brain activity in English-, French-, and Italian-speaking patients with developmental dyslexia. People with developmental dyslexia in all three countries showed decreased relative brain activity in the left superior temporal gyrus and the middle/inferior temporal gyrus, where altered brain activity was found in the previous studies. In summary, people with developmental dyslexia had reduced brain activity in the left occipito-temporal and temporo-parietal regions and increased brain activity in the inferior frontal gyrus. This was confirmed by a recent meta-analysis (Richlan, Kronbichler, & Wimmer, 2009). The dysfunction in the left temporo-parietal region is thought to be involved in grapheme-to-phoneme conversion (i.e., phonological

processing) for the following reasons. 1) Pseudo word reading produces stronger activation than real word reading. 2) This brain region is strongly activated during phonological tasks in healthy people whereas people with developmental dyslexia exhibit reduced activation in this brain region. In contrast, the left occipito-temporal cortex is thought to be responsible for “memory-based word identification” (Pugh et al., 2001). This is because word reading produces stronger left occipito-temporal cortex activation than pseudo word reading and leads to consistent activation across different tasks (e.g., phonological tasks and naming tasks). Because the left inferior frontal region is sensitive to pronunciation, this region may be involved in output phonology. Poor phonological processing in temporo-parietal regions may result in hyperactivation in the inferior frontal region (i.e., compensatory shift). What is the core deficit in developmental dyslexia? As reading acquisition can change brain anatomy and function, their causal relationship should be investigated. As noted, hyperactivation in the left inferior frontal region may reflect a compensatory shift. Additionally, some researchers have reasoned that dysfunction in the left occipito-temporal region is the result of poor reading exposure. Indeed, children with developmental dyslexia show disrupted brain activity in the left occipito-temporal cortex, activity in which is positively correlated with reading skill (Shaywitz et al., 2002). Another study directly revealed that reading acquisition changes cortical activity (Dehaene et al., 2010). The authors compared brain activity across illiterate adults, ex-illiterate adults, and skilled adults, and showed that there is greater activation in the left fusiform gyrus in ex-illiterate adults vs. illiterate adults. This implies that reading experience can change cortical activity. As cortical activity in the left occipito-temporal cortex is prompted by reading exposure, some

researchers have speculated that under activation of the left occipito-temporal region is a result of poor reading exposure. A recent study revealed the effects of reading exposure by systematically investigating the underlying mechanisms of hyper- and hypo-activation (Hoeft et al., 2007). The authors first confirmed the presence of reduced brain activity in the left inferior parietal lobule and the left fusiform gyrus, and increased cortical activity in the left inferior frontal gyrus. To rule out any effects of reading level on patients with developmental dyslexia and the control group, brain activity was compared between patients with developmental dyslexia and reading age-matched controls. In the left fusiform gyrus and the left inferior parietal lobule, the reading age-matched controls had greater activation than did patients with developmental dyslexia. There was no difference in the left inferior frontal gyrus. Thus, hyperactivity of the left inferior frontal gyrus may reflect current reading ability, while hypoactivity of the left fusiform gyrus which was found in comparison with age-matched control and the left inferior parietal lobule may originate from the neurobiological abnormality of developmental dyslexia.

Another study showed that the effects of literacy-related single-nucleotide polymorphisms in neurensin 1 (NRSN1), which is localized at 6p22 and may be involved in neuronal organelle transport, were distributed in brain regions including the left fusiform gyrus. The gray matter volume pattern in this brain region can successfully be used to distinguish between patients with developmental dyslexia and controls using multivariate pattern classification analysis (Michael et al., 2016). Thus, the left occipito-temporal region is skill-related brain region, however dysfunction in this region in developmental dyslexia cannot account only for poor reading experience.

Nonetheless, little is known about the underlying mechanisms of occipito-temporal dysfunction, as the core deficit in developmental dyslexia is thought to be phonological processing. Many researchers are committed to uncovering underlying mechanisms related to phonological processing. To better understand the underlying mechanisms of dysfunction of the occipito-temporal region during development, assessing brain function for language stimuli in the left occipito-temporal region in typically developing people seems important.

4. Visual word and character form processing in the brain

Letters are one of the great cultural inventions of the human primate. This invention is thought to have occurred around 5,400 A.C. When I consider the history of primates, the history of letters is not very long. This implies that the neuronal systems of reading might be organized by “recycling” other acquired brain functions (Dehaene & Cohen, 2007). Some studies have supported this cultural recycling hypothesis. There are empirical regularities in the shapes of letters and other human visual signs. Additionally, the configuration of the natural scene is highly similar to that of visual signs, including letters. This suggests that human visual signs have been developed to fit our visual system. If our visual word form system is developed based on the evolutionally older visual system, non-human primates may be able to learn orthographic rules. Baboons were trained to distinguish visually presented words and non-words (Grainger, Dufau, Montant, Ziegler, & Fagot, 2012). They are able to distinguish words from nonwords. The baboons did not simply memorize the words, because 1) nonword accuracy was significantly correlated with orthographic similarity, and 2) they could distinguish unlearned nonwords. This evidence implies that non-human primates can learn rules of visual word form system and that visual word form processing is not a language-specific process. Another study directly demonstrated that reading acquisition changes brain responses of visual stimuli (Dehaene et al., 2010). Literacy produced stronger activation in the left fusiform gyrus for written words and decreased activation for faces. This suggests that there is cortical organization following acquisition of reading ability. In summary, visual word form processing may be achieved by reorganizing brain systems used in visual processing, which share similar systems with

non-human primates. Neural mechanisms of visual system have been closely investigated in animals such as cats and monkeys. The primate visual system is considered to be divided into two pathways (Ungerleider G., 1982). The first is the dorsal visual pathway, which travels thorough early visual cortex, middle temporal area (MT), and middle superior temporal area (MST), and is devoted to spatial processing. The second is the ventral visual pathway, which passes through early visual areas and the anterior inferior temporal area (TE) and is involved in object identification. Since visual word forms are recognized in the ventral visual pathway, I will discuss how information is processed in this pathway. Felleman & Van Essen (1991) found a feed-forward projection from the retina to the lateral geniculate nucleus, and through the primary visual cortex (V1), the second visual cortex (V2), and the forth visual cortex (V4) to TE in monkeys. Similarly, diffusion tensor imaging (DTI) in humans can reveal a white matter tract passing through the ventral visual pathway (Yeatman, Rauschecker, & Wandell, 2013). Although the anatomical connections within the visual cortex are complicated, visual information travels from the posterior to the anterior direction in the brain. Parvocellular neurons in the lateral geniculate nucleus of the macaque produce response 56 msec after visual stimulus presentation. This is followed by V1 (67 msec) and V2 (82 msec) activity (Schmolesky et al., 1998). Additionally, neurons in the TE of the macaque are activated at approximately 100 msec, which is later than the response time observed in the visual cortex (Baylis, Rolls, & Leonard, 1987). Anatomical connections and neural responses time imply that visual information projected in the retina is processed through the lateral geniculate nucleus, V1, V2, V4, and the temporal cortex.

How is visual information processed in the ventral visual pathway? Neurophysiological studies show that the hierarchy of neurons is tuned to increasingly complex visual components throughout the ventral visual pathway. Neurons responding to specific orientations are found in V1, suggesting that this brain region is devoted to line orientation processing (Hubel & Wiesel, 1962). V2 neurons represent more complex shapes, such as angles, arcs, and circles (Hegdé & Van Essen, 2000; Ito & Komatsu, 2004). Another recent study showed that the V2 of the macaque monkey encodes combinations of orientations (Anzai, Peng, & Van Essen, 2007). Although the functions of V4 and the inferior temporal region in the macaque are not as well understood as those of V1 and V2 neurons, V4 and inferior temporal neurons respond to complex object features (Kobatake & Tanaka, 1994). The underlying mechanisms for encoding object features in the inferior temporal cortex are still debated (e.g., Brincat & Connor, 2004). However, it is likely that IT neurons encode more complex features compared to V1 and V2 neurons. As noted before, neural mechanisms of reading and object recognition are highly homogeneous. Dehaene et al. proposed the local combination detector (LCD) model, where multiple levels of information from a word (e.g., fragments, features, single letters, bigrams, quadrigrams, and the whole word) are hierarchically encoded, such that more anterior regions encode larger and more complex word components (Dehaene, Cohen, Sigman, & Vinckier, 2005). The LCD model was empirically examined using an alphabetic script (Vinckier et al., 2007). The authors exposed literate adults to (1) false fonts; (2) infrequent letters; (3) frequent letters; (4) frequent bigrams; (5) frequent quadrigrams; and (6) words. A posterior-to-anterior gradient was observed in the occipito-temporal cortex from (1) to (5). This supports the

LCD model.

Understanding neuronal mechanisms of visual character form processing for logographic characters is worth investigating for the following reasons. First, logographic characters have completely different surface forms compared to alphabetic scripts. Each character is a combination of radicals consisting of strokes. Second, children with developmental dyslexia in alphabetic script may have difficulties in hierarchical word form processing (van der Mark et al., 2011). Some studies have investigated visual processing of Chinese character using neuroimaging technique (Tan et al., 2001; Kuo et al., 2004). However, the underlying mechanism of logographic character recognition is not very well understood. Both Chinese and Japanese *Kanji* characters employ logographic strategies. The visual processing hierarchy of Chinese characters was investigated using real and pseudo Chinese characters and Korean Hangul (Chan et al., 2009). Since Korean Hangul has a simpler visual structure than real Chinese characters, the authors compared the two writing systems to assess the hierarchical visual processing of Chinese characters. Real Chinese characters activated the anterior part of the fusiform gyrus, while Korean Hangul activated the posterior fusiform gyrus in Chinese subjects. However, because the authors compared different languages, their findings may have been due to differences in structural components between the two languages (i.e., Chinese character and Korean Hangul). Another issue is that the participants were required to complete different tasks for the three types of stimuli (semantic vs. character form matching tasks). Therefore, the hierarchy demonstrated in the results might be dependent on the different cognitive strategies used, such that semantic processing is only recruited for real characters. Liu et al. (2008)

examined left occipito-temporal activations pattern for real, pseudo, and artificial Chinese characters. Although the activation peak in response to real Chinese characters were located in the more anterior part of the left occipito-temporal cortex relative to the peak for pseudo Chinese characters, the peaks for pseudo and artificial characters were also located in the same region. The methodological issue is that the radicals may have confounded the artificial Chinese character stimuli, resulting in the absence of contrast between the pseudo and artificial tasks. Thus, it has not been clearly demonstrated whether different visual components (e.g., stroke, radical, and whole character) of logographic characters, like as those used in Japanese *Kanji,* are processed in different brain regions in a hierarchical manner.

Japanese *Kanji* characters also employ logographic strategies. Investigating visual character form processing in logographic Japanese *Kanji* characters is important for the following reasons. First, the prevalence of developmental dyslexia for *Kanji* is quite high (Uno, Wydell, Haruhara, Kaneko, & Shinya, 2008). Although the prevalence of developmental dyslexia for *Hiragana* and *Katakana* reading have been shown to be 0.2% and 1.4%, respectively, 6.9% of children showed poor *Kanji* reading ability. As developmental dyslexia is a neurobiological disorder, uncovering neural substrates of logographic *Kanji* characters may have a critical role for better understanding the underlying mechanisms of *Kanji* reading deficits in people with developmental dyslexia. Second, Japanese consists of drastically different types of writing systems (i.e., syllabic *Kana* and logographic *Kanji*). This enabled me to directly evaluate how different and/or similar visual forms of syllabic and logographic systems are recognized in our brain. Comparing neural representations across different writing systems may contribute to

discovering biological unity and evolutional changes required for reading. To study this issue, I investigated visual form processing of logographic Japanese *Kanji* characters.

Chapter II Purpose

Impaired visual word form processing is one of the critical symptoms of developmental dyslexia, although the underlying neural mechanisms are not well understood. To uncover altered neural substrates of visual processing in people with developmental dyslexia, I need to know how the visual word and/or character forms are recognized in typically developing children beforehand.

Neural mechanisms of visual word form processing have been closely investigated for alphabetic scripts, but neural substrates of visual processing for non-alphabetic scripts such as Japanese *Kanji* are poorly understood. As Japanese *Kanji* characters have completely different surface forms compared to alphabetic letters and employs logographic strategies, it seems important to investigate how the visual forms of Japanese *Kanji* characters are processed in the brain. Japanese *Kanji* characters consist of hierarchical structures, such as strokes, radicals, and whole characters, and behavioral studies imply that these structures have some influence on reading. Because alphabetic words are processed hierarchically from posterior to anterior in the left ventral visual pathway such that lower cognitive components (e.g., letters) are recognized in the posterior part and higher cognitive components (e.g., words) are processed in the anterior part (Vinckier et al., 2007), I hypothesized that Japanese *Kanji* characters are hierarchically recognized in the left ventral visual pathway.

To uncover hierarchical visual character form processing of Japanese *Kanji* characters, I used functional magnetic resonance imaging (fMRI). In the first experiment, I examined how different hierarchical structures of Japanese *Kanji*

characters activate the ventral visual pathway. As Japanese *Kanji* characters are visually complex and look similar to objects, I need to examine whether such characters are processed like alphabetic words or objects. In the second experiment, I thus applied a similar procedure to objects to compare brain activation patterns between objects and *Kanji* characters. In sum, I examined how the visual character forms of Japanese *Kanji* characters are represented in the left ventral visual pathway and whether this hierarchical representation pattern is similar to that of objects throughout these experiments.

Chapter III Experiment 1: Visual form processing of Japanese *Kanji* character

1. Purpose

Japanese *Kanji* characters consist of a hierarchical structure, such as strokes, radicals, and whole characters. These hierarchical visual structures may produce different spatial distribution patterns within occipito-temporal cortices. Some behavioral studies imply that reading Japanese *Kanji* characters involves hierarchical processing of subcomponents (i.e., strokes and radicals) (e.g., Saito et al., 1999; Tamaoka & Yamada, 2000); however, the hierarchical visual processing of Japanese *Kanji* characters has not been assessed by neuroscientific methods. To uncover hierarchical visual processing, I will expose participants to (1) real *Kanji* characters (complete structures of characters), (2) pseudo *Kanji* characters (legitimate at the radical level), (3) artificial characters (containing strokes), and (4) checkerboard (optical component), and measure the brain activation for these stimuli using fMRI based on Liu et al. (2008)'s study . In this experiment, I will examine whether *Kanji* characters are processed hierarchically from posterior to anterior in the left occipito-temporal cortex by comparing the spatial distribution patterns for these stimuli.

2. Materials and Methods

2.1. Participants

Twenty-eight right-handed healthy native Japanese speakers (mean age = 21.7 years, SD = 2.3 years, age range: 18–28 years, 13 males, 15 females) with normal or

corrected vision and without language or speech impediments participated in the present study. Their handedness was affirmed with the Edinburgh handedness inventory (Oldfield, 1971). I excluded 5 of the original 33 participants from the analyses because they failed to respond to the stimuli more than 5 times per session in all sessions. All participants were undergraduate or graduate students who were already qualified by entrance exam to the universities, so that they are supposed to have sufficient sight word reading ability. This study was approved by Research and Ethical Committee of University of Tsukuba and National Center of Neurology and Psychiatry, and written informed consent was obtained from each participant prior to the study.

2.2. Stimuli

I showed 1) real *Kanji*, 2) pseudo *Kanji*, 3) artificial character, and 4) a checkerboard stimuli (Figure 4A). Eighty *Kanji* characters with 8–12 strokes were chosen for the real *Kanji* character stimuli. In this study, a psycholinguistic database of lexical properties of Japanese (Amano & Kondo, 2003) was used to examine the familiarity and frequency of these *Kanji* characters. This database includes subjective rating data for word familiarity, character familiarity, and visual complexity. For objective scale, this database contains word and character frequency in the newspaper. I collected highly familiar and frequent characters (>1 SD from the mean in the database) because these characters are used frequently in daily life. Additionally, all *Kanji* characters were chosen from 2136 daily used *Kanji* which Japanese students commonly learn to read and write. This may attenuate startle effect of the stimuli. Both pseudo *Kanji* and artificial characters were made by recomposing subcomponents of real *Kanji*

characters. Pseudo *Kanji* characters were made by replacing the subcomponents of a real *Kanji* character with a radical of another real *Kanji*, such that the pseudo *Kanji* stimuli include real subcomponents but are not fully structured as real *Kanji* characters. I prepared artificial characters by decomposing *Kanji* subcomponents first and then randomly recomposing them. Hence, artificial characters were unpronounceable, meaningless, and never included *Kanji* subcomponents. Thus, unlike the study by Liu et al. (2008), I decomposed artificial characters into a completely non-linguistic level, which enabled us to evaluate whether *Kanji* characters and subcomponents would activate different brain regions within the left occipito-temporal cortex. Half of the stimuli were 20% larger in terms of size than the other half, so I obtained even sets of "large" and "small" characters. All stimuli are found in Appendix A.

2.3. Experimental Design

The participants were put in the scanner and then experienced four consecutive fMRI sessions, each of which consisted of 20 real *Kanji* characters, 20 pseudo *Kanji* characters, 20 artificial characters, and 20 checkerboard stimuli. Each stimulus was exposed to 600 ms, followed by the presentation of a fixation cross (Figure 4B). The length of presentation of the fixation cross was randomized to be between 2.5 and 12.5 s. In a typical BOLD response, the response peaks roughly 5 s after stimulation, followed by an undershoot at approximately 15 s (Malonek et al., 1997). To purely measure brain activity for each event, stimuli would need to be provided roughly every 20 s. However, this would require a long time to complete the task, and this is not realistic for human experiments. Nowadays, hemodynamic responses can be decoded when inter stimulus

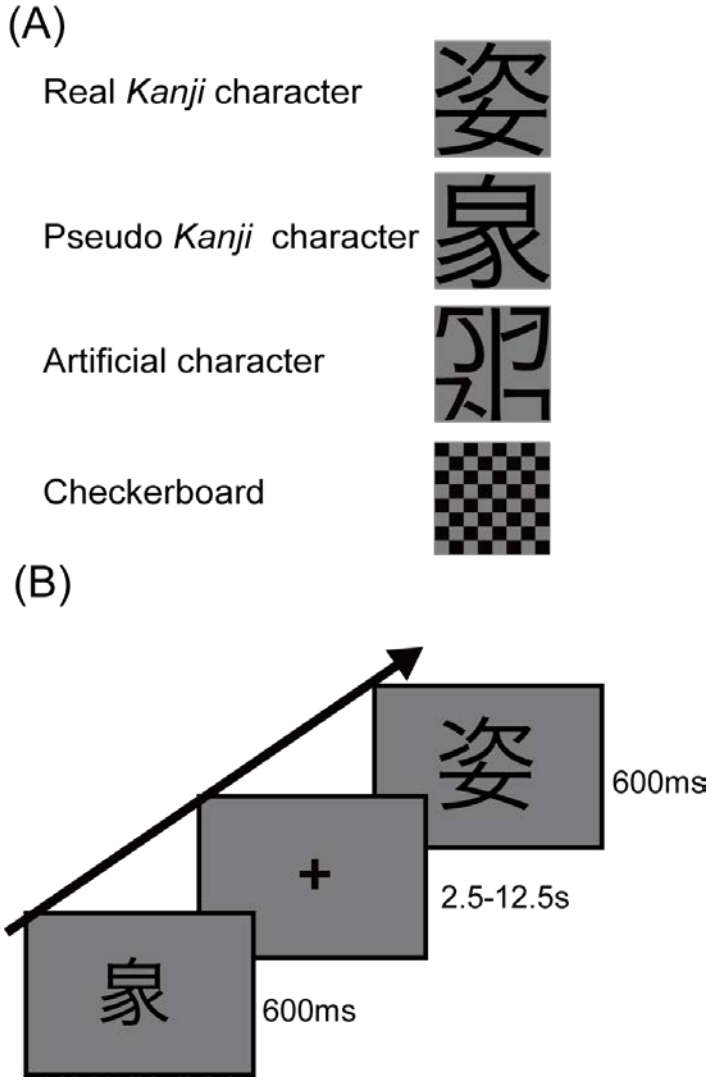

Figure 4 Stimuli examples and schematic illustration of the experimental design. (A) This figure shows four types of presented stimuli. We exposed real *Kanji* characters (complete structure), pseudo *Kanji* characters (random combinations of subcomponents), artificial characters (character fragments), and a checkerboard (simple photic stimuli). (B) During the fMRI session, participants were required to judge if the presented stimuli were larger or smaller.

intervals (ISI) are randomly jittered, and an ISI around 5 to 15 s has been widely used (Henson & Friston, 2007). The orders of the four types of stimuli were randomized across sessions. According to a previous study (Liu et al., 2008), I used a size judgment task. Participants were required to judge the size of a character (large or small) for each event and press a response button with their right index or middle finger if the stimulus was large or small, respectively. Large characters were 20% larger than small characters. As I used only two sizes of stimuli, participants were trained before the fMRI in the scanner so that they could distinguish the stimuli as large or small. During the fixation periods, participants maintained their gaze on the fixation point without providing any responses. Sessions in which the participant did not respond for more than five times were excluded from analysis. The experimental paradigm was controlled by the Presentation software (Neurobehavioral Systems, Berkeley, USA).

2.4. fMRI data acquisition and analysis

2.4.1. fMRI acquisition

I obtained functional echo planar images (EPI) using a Siemens (Erlangen, Germany) 1.5-Tesla MRI system (TR = 2500 ms, TE = 40 ms, flip angle 90°, 4-mm-thick axial slices, in-plane resolution = 3.4 × 3.4 mm). The time-series of functional data of 190 whole-brain 3D EPI volumes were acquired in each session. After functional image acquisition, a T1-weighted high-resolution anatomical image was obtained (TR = 1900 ms, TE = 3.93 ms, flip angle 15°, voxel size = 1.4 × 1.0 × 1.3 mm).

2.4.2. fMRI data analysis

I analyzed the functional imaging data using SPM8 (Wellcome Department of Cognitive Neurology, London, UK, http://fil.ion.ucl.ac.uk/spm/). The first five images were excluded from further analyses to avoid T1 equilibration effects. To compensate the differential temporal offsets between slices, I applied slice-timing correction to the images. Then I spatially realigned the functional images to the first image for motion correction and coregistered the functional images to the individual structural image (high-resolution T1). The individual structural image was spatially normalized to the MNI T1 template image. By using the resulting normalization parameters, all functional images were spatially normalized. Finally, functional images were smoothed using a Gaussian filter (6-mm FWHM).

To model the hemodynamic time series in each condition, I convolved the stimulus presentation time (600 ms) with the canonical hemodynamic response function (HRF). Individual hemodynamic changes for each of four types of stimulus events (real *Kanji*, pseudo *Kanji*, and artificial characters and checkerboard) were assessed using a session-wise general linear model that included the linear combination of the regressors for the hypothetical hemodynamic responses to the four types of events, motion parameters, and high-pass filtering regressors (128 s). I estimated the parameters (beta-weights) for the four conditions, and the parameters were fed into the group analysis.

First, I identified which parts of the brain were differentially activated by the four types of stimuli (real *Kanji* character, pseudo *Kanji* character, artificial *Kanji* character, and checkerboard). All beta-weight maps for the four conditions were

compared using one-way repeated measures analysis of variance (ANOVA). The height threshold was set at $p < 0.005$ (uncorrected), and the cluster size threshold was $p < 0.05$ (corrected with family wise error [FWE]; 536 or more voxels). Finally, I investigated the differential loci of the peak activation for the three stimulus conditions to see if there was a topologically hierarchical peak distribution. The beta-weight maps for the three stimulus conditions were compared using one-way repeated measures ANOVA. For this analysis, the height statistical threshold was set at $p < 0.001$, uncorrected, and the cluster size threshold was set at $p < 0.05$ with FWE corrected (463 or more voxels).

2.4.3. Region of interest analysis

To differentiate spatial patterns of activation for real *Kanji*, pseudo *Kanji*, and artificial characters, five non-overlapping regions of interest (ROIs) were defined based on the previous study (van der Mark et al., 2009). These ROIs cover the putative VWFA and the neighboring region. Each spherical ROI had a 3-mm radius, and all the ROIs were located along with the posterior-anterior axis (slightly declined toward the anterior direction). The center coordinates for the ROIs are as follows: (MNI coordinate [x, y, z] in mm) ROI1 (−45, −75, −12), ROI2 (−45, −67, −13), ROI3 (−45, −59, −14), ROI4 (−45, −51, −15), and ROI5 (−45, −43, −16). ROI3 was located on the proper VWFA region for Japanese *Kanji* that was described in the previous meta-analysis of culturally specific word regions (Bolger, Perfetti, & Schneider, 2005). Similarly, contralateral coordinates were defined as center coordinate for ROIs of the right occipito-temporal cortex. The ROI definition and parameter estimates were conducted using the MarsBaR toolbox (http://marsbar.sourceforge.net). In the ROI analysis, I extracted contrast

estimates for each contrast. As noted in the fMRI data analysis, I calculated beta images of stimuli types (i.e., real *Kanji* character, pseudo *Kanji* character, artificial *Kanji* character, and artificial character). Calculated beta images were fed into the general linier model, and contrasts were estimated as a linear combination of these variables. This linear combination of estimated beta values is the contrast estimate I used in the ROI analysis.

3. Results

3.1. Behavioral data of the size judgment task

Correct response rate of all conditions was almost 100% (Figure 5). Indeed, size judgment task accuracy did not differ significantly between different character sizes (large or small) or types (real, pseudo, artificial, or checkerboard), $F(1, 27) = 1.34$, $p = 0.257$ and $F(1.4, 38.2) = 5.04$, $p = 0.020$ respectively. I found significant interactive effect of size × types, $F(1.62, 27) = 8.94$, $p = 0.001$, such that, although correct response rate in response to large and small stimuli is mostly identical to each other on four types of stimuli, correct response rate to large stimuli (98.3%) was a little lower than that to small stimuli (99.6%) on the checkerboard condition. I cannot put the plausible explanation for this lower correct response rate judging larger checkerboard, but there were no interactive effect of size × type at least within three character types on correct response rate [$F(2,54) = 0.216$, $p = 0.806$].

The reaction time did not significantly differ between the character sizes (large or small) and types (real, pseudo, artificial, or checkerboard), $F(1, 27) = 4.25$, $p = 0.049$ and $F(3, 81) = 1.31$, $p = 0.278$ respectively. There was an interactive effect of size × type on the reaction time, however, $F(1.8, 49.6) = 7.11$, $p = 0.002$, such that participants responded faster to larger character stimuli than smaller characters although they responded slower to larger checkerboard stimuli than to smaller checkerboards (Figure 6). As in the case with the interactive effect on accuracy, I could not find any interpretable reason for this interaction on reaction time. But there were no interactive

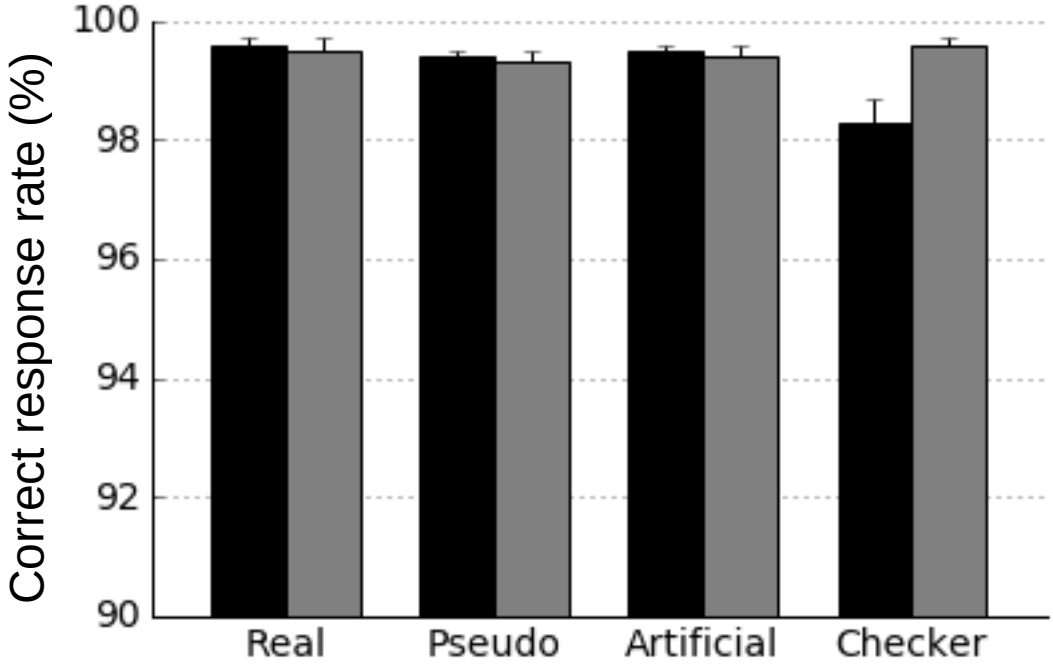

Figure 5 Correct response rate for real *Kanji* character, pseudo *Kanji* character, artificial character, and checkerboard stimuli. The values are the mean ± SEM (n = 28). Correct response error rate for large stimuli are colored in black, and small stimuli are colored in gray.

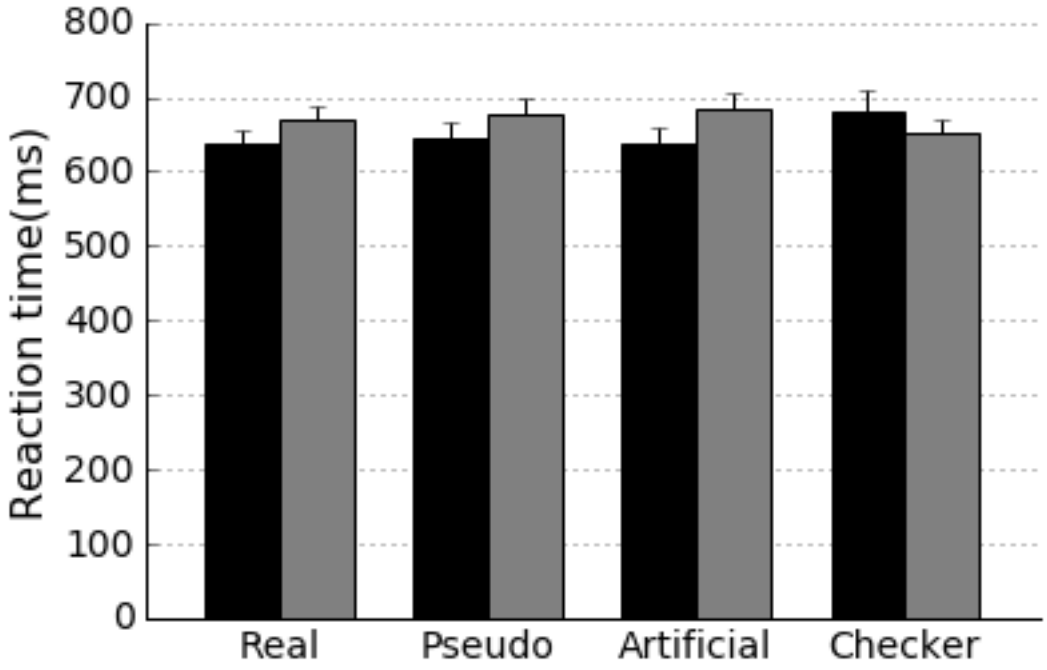

Figure 6 Reaction times for real *Kanji* character, pseudo *Kanji* character, artificial character, and checkerboard stimuli. The values are the mean ± SEM (n = 28). Reaction times for large stimuli are colored in black, and small stimuli are colored in gray.

effect of size × type within three character types on reaction time [$F(2,54) = 0.417$, $p = 0.661$]. Therefore, participants performed equally in terms of response accuracy and speed, at least for the three character types of stimuli that are focus of our study. Because size judgement is not a scope of this study, both big and small size conditions were fed into the same conditions in the fMRI analysis.

3.2. fMRI data

3.2.1. Differently activated brain region among all types of stimuli

To identify main effects of stimuli (real *Kanji* character, pseudo *Kanji* character, artificial characters, and checkerboard), brain activity was analyzed using a one-way repeated measures ANOVA (Figure 7 and Table 2). Bilateral occipito-temporal cortices including the inferior temporal gyrus and inferior occipital gyrus were differently activated in response to the real *Kanji*, pseudo *Kanji*, artificial characters, and checkerboard stimuli. I was able to confirm that the four types of stimuli differentially activated the bilateral occipital gyrus and fusiform gyrus.

3.2.2. Brain activity for each types of Kanji characters

To investigate brain activity for each type of *Kanji* character, I mapped brain activity for real *Kanji*, pseudo *Kanji*, and artificial character stimuli in comparison to the checkerboard stimuli (Figure 8 and Table 3). Real *Kanji* characters activated bilateral occipito-temporal cortex, including fusiform and inferior temporal gyri. A similar activation pattern was observed for pseudo *Kanji* and artificial characters. These characters activated similar brain regions; however, the peak regions for the artificial,

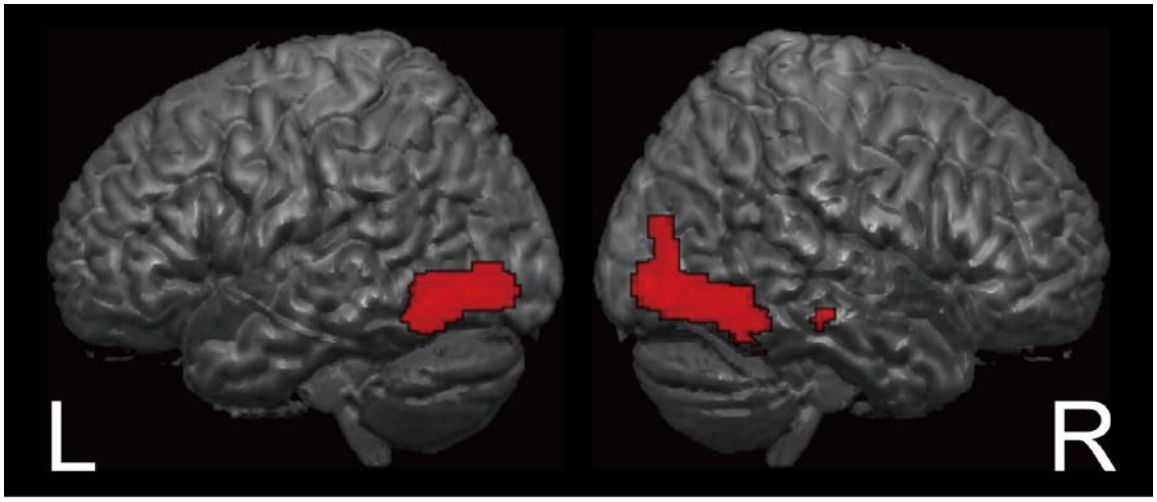

Figure 7 Brain activity showing the main effect of stimuli (real *Kanji* characters, pseudo *Kanji* characters, artificial characters, and checkerboard). Bilateral occipito-temporal cortices were differentially activated between the real *Kanji*, pseudo *Kanji*, artificial characters, and checkerboard. The height threshold for illustration was $p < 0.005$, (uncorrected), with a cluster-size threshold of $p < 0.05$ (corrected) with family wise error (FWE, 536 or more voxels).

Table 2 Differentially activated brain region among the real *Kanji* characters, pseudo *Kanji* characters, artificial characters, and checkerboard.

Region	MNI Coordinates (mm)			*F*	voxels	BA
	x	y	z			
R Inferior Temporal Gyrus	44	-66	-10	33.67 **	1464	37
R Inferior Occipital Gyrus	40	-80	-8	26.75 **		19
R Inferior Temporal Gyrus	46	-56	-12	20.38 **		37
L Inferior Temporal Gyrus	-48	-64	-10	27.51 **	1338	37
L Inferior Occipital Gyrus	-40	-80	-6	19.14 **		19
L Inferior Temporal Gyrus	-42	-48	-14	9.15 *		37

*$P < 0.005$, cluster size threshold of $P < 0.05$ (FWE corrected) ** $P < 0.05$ (FWE corrected) for the height threshold.

This table shows differentially activated brain regions between the real *Kanji*, pseudo *Kanji*, artificial *Kanji*, and checkerboard stimuli. Bilateral occipito-temporal cortices were differentially activated.

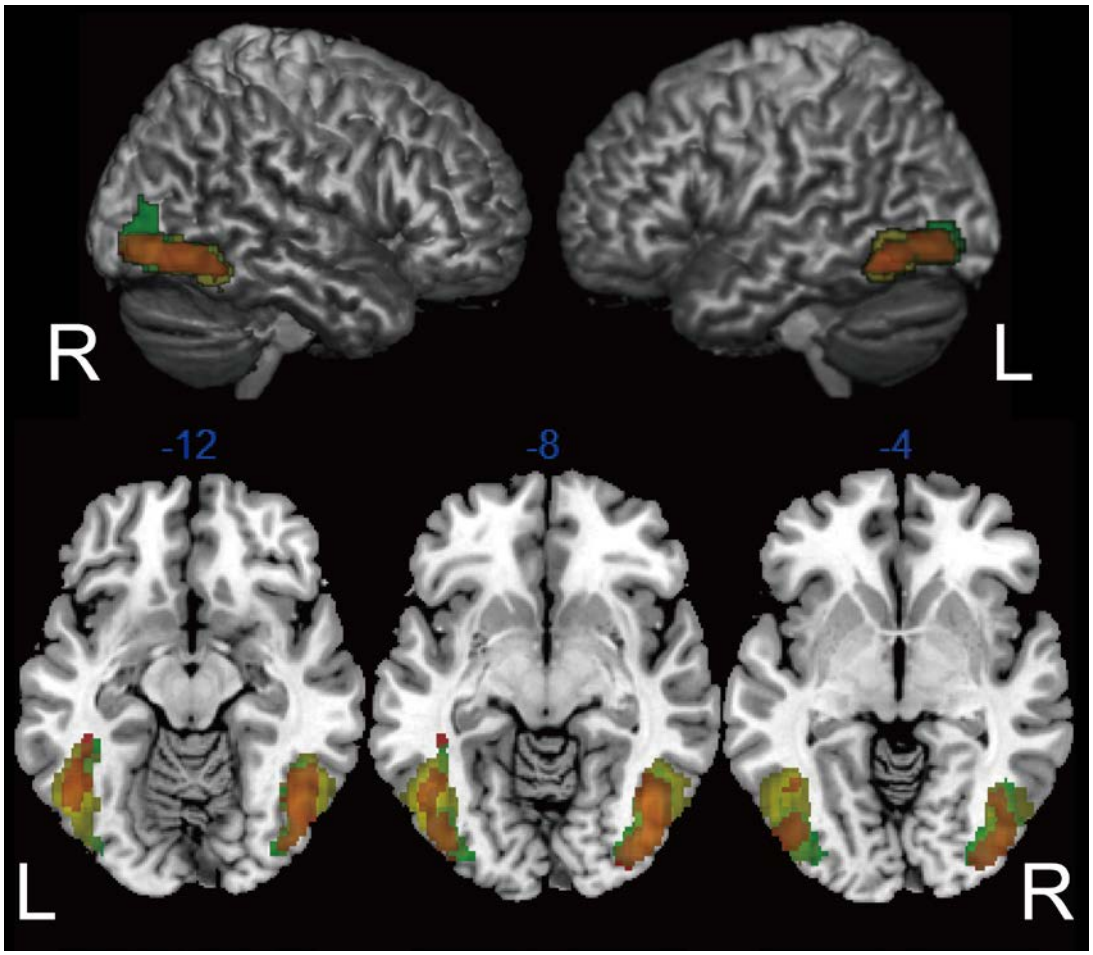

Figure 8 Activated brain region for real *Kanji*, pseudo *Kanji*, and artificial characters in comparison to checkerboard. The height threshold was set at $p < 0.005$ with cluster level threshold $p < 0.05$ (FWE corrected). The brain activity for real *Kanji* are colored in red, pseudo *Kanji* are colored in yellow, and artificial character are colored in green. I found these characters significantly activate bilateral occipito-temporal cortices.

Table 3 Brain regions activated by each stimulus type

Region	MNI coordinates (mm)			*T*		voxels	BA
	x	*y*	*z*				
Real > Checkerboard							
R inferior temporal gyrus	42	−66	−10	6.56	*	713	37
R inferior occipital gyrus	40	−82	−8	5.86	*		19
R fusiform gyrus	48	−52	−14	4.50	*		37
L fusiform gyrus	−44	−58	−12	4.83	*	463	37
L inferior occipital gyrus	−40	−78	−6	4.72	*		19
L sub-gyral	−42	−40	−10	4.01	*		37
Pseudo > Checkerboard							
R inferior temporal gyrus	44	−66	−10	9.70	**	1353	37
R inferior occipital gyrus	42	−78	−8	8.02	**		19
R fusiform gyrus	46	−56	−12	7.68	**		37
L inferior temporal gyrus	−48	−64	−10	8.89	**	1342	37
L inferior occipital gyrus	−40	−80	−6	6.54	**		19
L fusiform gyrus	−36	−42	−22	4.48	*		20
Artificial > Checkerboard							
R inferior occipital gyrus	38	−82	−8	7.63	*	1033	19
R middle temporal gyrus	42	−64	−8	7.23	*		37

L inferior occipital gyrus	−40	−80	−6	6.55	*	522	19
L fusiform gyrus	−40	−44	−12	3.89	*		37
L fusiform gyrus	−42	−54	−10	3.76	*		37

* $P < 0.001$ (uncorrected), cluster siz e threshold of $P < 0.05$ (FWE corrected) **$P < 0.05$ (FWE corrected) for the height threshold.

pseudo *Kanji*, and real *Kanji* characters appeared to be located in the left occipito-temporal cortex in a posterior to anterior order. In the left occipito-temporal cortex, peak loci for artificial, pseudo *Kanji*, and real *Kanji* characters were in the inferior occipital gyrus ($x = -40$, $y = -80$, $z = -6$), inferior temporal gyrus ($x = -48$, $y = -64$, $z = -10$), and fusiform gyrus ($x = -44$, $y = -58$, $z = -12$). Conversely, in the right occipito-temporal cortex, the peak locations for real ($x = 42$, $y = -66$, $z = -10$) and pseudo *Kanji* characters ($x = 44$, $y = -66$ m $z = -10$) were adjacent to each other. This analysis suggests that hierarchical localization of the activations was dominant in the left side of the occipito-temporal cortex.

3.2.3. Different spatial patterns of activation within the left occipito-temporal cortex for all Kanji character types

My previous analysis showed real *Kanji*, pseudo *Kanji*, and artificial characters activate bilateral occipito-temporal cortices. However, these characters may produce different spatial distribution patterns within the occipito-temporal cortices. To test this hypothesis, I created consecutive ROIs within the region and compared the spatial patterns of activation across the three conditions (Figure 9). First, a three-way repeated measures ANOVA of contrast estimates showed significant main effects of laterality, ROI locations (1–5), and character types (real *Kanji* character, pseudo *Kanji* character, and artificial character; $F(1, 27) = 20.76$, $p < 0.001$, $F(4, 108) = 14.29$, $p < 0.001$, and $F(2, 54) = 4.87$, $p = 0.011$, respectively). This result implies different brain activation patterns between the left and right occipito-temporal cortex. As the purpose of this ROI analysis was to examine whether character types produced different spatial distribution

patterns, I next investigated interactive effects of ROI locations and character types. A two-way repeated measures ANOVA of the contrast estimate of activations revealed an interactive effect of ROI locations (1–5) × character types (real, pseudo, and artificial; $F(8,216) = 3.847$, $p = 0.009$). This interaction was explained by the differential spatial distributions (i.e., different locations for the most activated ROI) across the three types of characters in the left side of occipito-temporal cortex (Fig. 9, left). For artificial characters, the most activated ROI was in the extreme posterior region (ROI1), and brain activity was decreased along the posterior-anterior axis. Pseudo *Kanji* characters evoked the strongest activity in the second ROI from the posterior region (ROI2). Conversely, real *Kanji* characters elicited the strongest activity in the middle ROI (ROI3), which corresponds to the putative center of the VWFA for Japanese *Kanji* characters. In the right occipito-temporal cortex, however, I did not find an interactive effect of ROI locations (1–5) × character types (real, pseudo, and artificial). This is because activity for the three types of stimuli linearly decreased from posterior ROIs to anterior ROIs in the right occipito-temporal cortex. As expected, the result strongly supports the hypothesis that artificial, pseudo *Kanji*, and real *Kanji* characters are processed hierarchically from posterior to anterior in the left occipito-temporal cortex.

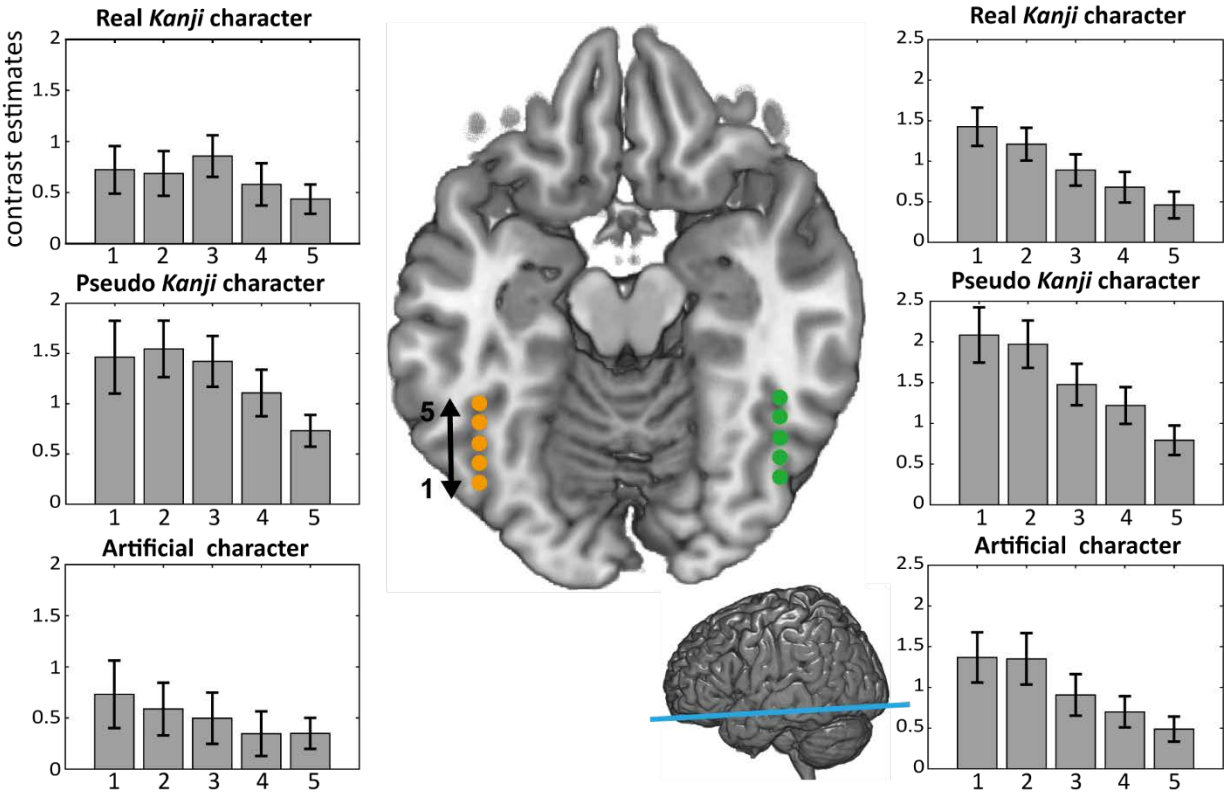

Figure 9 ROI analysis in the bilateral occipito-temporal cortices. The consecutive numbers 1–5 on the brain slice section indicate the ROI number, such that the most posterior ROI is numbered 1 (ROI1) and the most anterior ROI is numbered 5 (ROI5) in the occipito-temporal cortex along the posterior-anterior axis (blue line on the bottom figure). The three bar graphs show the contrast estimates (a.u.) of the neural activity in ROIs 1–5 in response to real *Kanji*, pseudo *Kanji*, and artificial characters. The error bars represent standard errors across participants. Orange and green circle shows ROIs for left and right occipito-temporal cortex, respectively.

4. Discussion

The purpose of the present study was to examine whether the visual forms of Japanese *Kanji* characters are processed hierarchically in the brain. The peak loci for real *Kanji,* pseudo *Kanji*, and artificial character were aligned from posterior to anterior within the left occipito-temporal cortex, however peak loci for real *Kanji*, and pseudo *Kanji* were overlapped within the right occipito-temporal cortex. The ROI analysis of the left occipito-temporal cortex statistically confirmed my hypothesis such that the spatial activation patterns (i.e., the patterns of activations across five consecutive ROIs) were different between the stimulus types and the most activated ROIs for the three stimulus types lined up in order.

Neural substrates of visual form processing have been assessed in the logographic script for Chinese characters. My previous study was based on the study by Liu et al. (2008). In contrast with the parameters in my experiments, peak loci for pseudo and artificial characters were overlapped in Liu et al. A plausible reason is that character-like stimuli were used as an artificial character in Liu et al, and characters were not decomposed to the stroke level. Contrastingly, artificial characters used in my experiments were decomposed to the stroke level. As the focus of their study was not to investigate hierarchical processing of logographic characters, Liu et al did not carry out ROI analysis. In relation to this study, it is not possible to compare hierarchical character form processing between Japanese *Kanji* and Chinese character. Another study exposed participants to Chinese characters, pseudo Chinese characters, and Korean Hangul. It was found that the anterior ROI exhibits strong activation for Chinese

characters; whereas, the posterior ROI strongly responds to Korean Hangul. It was stated that this result is an evidence for hierarchical processing of Chinese characters; however, different scripts of stimuli were used in the study. Thus, it seems reasonable to postulate that this difference is induced by the brain activity for the first and unlearned language. Thus, to the best of my knowledge, my experiment is the first to imply that the hierarchical components of logographic characters are hierarchically recognized in the left occipito-temporal cortex.

Some studies have shown hierarchical activation for visual word forms in the left occipito-temporal cortex for alphabetic script (Vinckier et al., 2007; Thesen et al. (2012). For instance, Thesen et al. (2012) showed real words, pseudo words, and false fonts to participants in the scanner and observed hierarchical organization of the left fusiform gyrus. Pseudo words are meaningless but contain real letters. However, false fonts contain letter-like symbols, so the authors reasoned that letter forms would be indexed by the contrast of pseudo word versus false fonts, whereas word forms would be indexed by the contrast of real words versus pseudo words. They also performed magnetoencephalography (MEG) and observed a letter-selective response occurring 60 ms earlier than the word-selective response, strongly suggest that “letter” information is processed prior to the “word” information in the left occipito-temporal cortex. Although I found interaction between ROIs and stimulus types, interpretation of this interaction remains only descriptive. However, it is reasonable to think that results indicate hierarchical organization of Japanese *Kanji* character, which is similar to hierarchical word form processing of alphabetic script.

Due to the visual complexity of Japanese *Kanji* characters, one fMRI study suggested that right lateralized brain activation for Japanese *Kanji* character (Nakamura et al., 2005). In the present study, however, I observed a different spatial distribution pattern of the brain activation in the left occipito-temporal cortex. Evidence from brain lesion studies supports our hypothesis of the dominance of the left hemisphere for visual processing, even for Japanese *Kanji*; lesions in the left inferior temporal area cause alexia with agraphia for Japanese *Kanji* characters (Iwata, 1984), and patients with damage to the left inferior temporal region exhibit poor lexical decision performance (Tani, 2004). In addition, Korean cerebrovascular disease patients with damage to the left inferior temporal region show decreased performance when reading logographic Hanja (Korean logographic character) (Kwon et al., 2002). Collectively, the existing evidence indicates that visual forms of logographic characters including Japanese *Kanji* may be processed in the same manner in the left hemisphere as alphabetic scripts.

Another aspect to be concerned is the semantic and phonological information which each Japanese *Kanji* character has. Recent neuroimaging studies have shown that the left fusiform gyrus is involved in phonological processing (Dietz, Jones, Gareau, Zeffiro, & Eden, 2005). The Japanese *Kanji* characters I used in this study can be read aloud, while pseudo *Kanji* and artificial characters do not contain phonological information at the whole character level. The different activation peak loci for the three types of *Kanji* character might be due to differences in phonological processing induced by the three types of characters. However, a neuroimaging study showed that brain activity for pseudo word was larger than that for real words in the left occipito-temporal cortex (Dietz et al., 2005). Reading pseudowords requires grapheme to phoneme

conversion, although reading real word can be achieved by using lexical knowledge. This implies that activation related to phonological processing in the left fusiform gyrus is supposed to be task dependent. Similarly, semantic information might induce different loci of peak activation in the left occipito-temporal cortex, because real *Kanji* characters I used were highly familiar ones which perhaps easily activate semantic networks. In the present study, I exposed each stimulus promptly (600 ms) and I required the participants to judge the size of the stimulus in order to minimize the participants' time to read the stimulus with their "internal voice" or to recruit semantics of the stimuli. Nevertheless, the different phonological and/or semantic information between the character types (real *Kanji*, pseudo *Kanji*, and artificial character) could have affected activity in the left occipito-temporal cortex to some extent. More generally, however, the existence of semantic and phonological information in each Japanese *Kanji* character is a nature of this writing system, and these characters no longer have any meaning as language stimuli without semantic and phonological information.

Although I found different spatial distribution pattern in the left occipito-temporal region, pseudo *Kanji* character produced stronger activation than real *Kanji* and artificial character. One of the conceivable possibilities of this strong activation is the novelty of the visual stimuli. Some researchers reported that novel objects activates the fusiform gyrus more than familiar objects (Zhang, Liu, & Zhang, 2013). Considering that pseudo characters created in this study do not exist in reality, these characters are supposed to be more novel than real *Kanji* characters. Thus, the novelty of pseudo *Kanji* characters may induce more brain activity. Moreover, I could speculate that phonological processing may have some influence on brain activation in

the left occipito-temporal cortex. As I stated in the general introduction, pronunciation of Japanese *Kanji* characters is derived from pronunciation of phonological radicals. For example, the Japanese *Kanji* character “校”, which is pronounced /kou/, is consistent with the pronunciation of the phonological radical “交” (/kou/). I made pseudo *Kanji* characters by reconstructing radicals, and some pseudo *Kanji* characters contain phonological radicals. Thus, I could not exclude the involvement of phonological processing for the brain activity in the left occipito-temporal cortex. Further studies are needed to clarify speculative ideas, such as the effect on visual word processing of stimulus novelty and subjects’ implicit attempts to pronounce pseudo *Kanji* characters with multiple pronounceable subcomponents.

In summary, I found that real *Kanji*, pseudo *Kanji*, and artificial characters activate the left occipito-temporal cortex from posterior to anterior in order. Peak loci analysis for the three types of characters in comparison to checkerboard stimuli in the left occipito-temporal cortex revealed that these characters activate different brain regions, such that peak loci for real *Kanji*, pseudo *Kanji*, and artificial characters are the fusiform gyrus, inferior temporal gyrus, inferior occipital gyrus, respectively. However, I found peak loci for both real *Kanji* and pseudo *Kanji* characters in the inferior temporal gyrus. Moreover, peak loci for real *Kanji*, pseudo *Kanji*, and artificial *character* were lined up from posterior to anterior within the left occipito-temporal cortex. However, peak loci for real *Kanji* and artificial characters overlapped. This result was also confirmed by the ROI analysis. A significant interaction was seen between the ROIs placed on the posterior-to-anterior axis in the left occipito-temporal cortex and stimulus types (i.e., real *Kanji*, pseudo *Kanji*, and artificial characters) within

the left occipito-temporal cortex. However, this interaction was not found in the right occipito-temporal cortex. The interactive effect in the left occipito-temporal cortex reflects a difference in spatial distribution patterns depending on the stimulus type, such that ROIs that showed the largest activity were aligned along the posterior to anterior axis in the following order: those for artificial characters (ROI1), pseudo *Kanji* (ROI2), and real *Kanji* characters (ROI3). This systematic difference in spatial distribution patterns may reflect the hierarchical processing of Japanese *Kanji* characters.

Chapter IV Experiment 2: Visual processing of objects

1. Purpose

Our first experiment implies visual forms of Japanese *Kanji* characters are hierarchically recognized in the left occipito-temporal cortex. Basic cognitive processes for word and character form recognition seem to be similar to the object recognition system, as I discussed in the introduction. Additionally, surface forms of Japanese *Kanji* characters are complex compared with alphabetic letters, and may have quite similar visual structures to objects. Thus, the different spatial distribution patterns in the left occipito-temporal cortex for Japanese *Kanji* characters may simply reflect brain responses to complex visual objects. In this second experiment, I aim to uncover whether hierarchical processing of Japanese *Kanji* characters is similar to object recognition, and I measured brain activity evoked by the following stimuli: (1) real objects (complete structures of objects), (2) pseudo objects (containing subcomponents of objects), (3) artificial patterns (containing fragments of objects), and (4) controls (simple optical components). By illustrating the spatial distribution of brain activity for these stimuli, I examined whether the hierarchical brain activation pattern for Japanese *Kanji* characters is similar to that for objects.

2. Materials and Methods

2.1. Participants

A total of eighteen right-handed healthy native Japanese speakers (mean age = 23.0 years, SD = 3.1 years, age range: 20–32 years, 9 males, 9 females) with normal or

corrected vision and without language or speech impediments participated in the present study. Their handedness was confirmed using the Edinburgh handedness inventory (Oldfield, 1971). Experimental procedure was approved by Research and Ethical Committee of University of Tsukuba and National Institute of Advanced Industrial Science and Technology, and written informed consent was obtained from each participant prior to the study.

2.2. Stimuli

The stimuli of this experiment were created in a similar manner to the experiment of the *Kanji* character (Experiment 1). I showed illustration of 1) a real object, 2) a pseudo object, 3) an artificial pattern, and 4) control stimuli. (Figure 10A). The real objects were line drawings that were taken from the web page of free-use illustration (http://www.printout.jp/clipart/). These included familiar objects such as vehicles, kitchen goods, stationery, and foods. All of the images were gray-scaled to exclude the effect of color. Pseudo objects were created by decomposing the components of real objects (e.g., the handle of mugs) and then reconstructing these decomposed components. These objects were legitimate at the component level but do not exist at a whole object level. Artificial patterns were created using in-house script written in MATLAB (The Mathworks, Massachusetts, USA) such that these stimuli only contained fragments of objects (e.g., angle and cross) but did not have information about the components of the objects. Artificial patterns were created by breaking them into real objects and reconstructed these broken columns. However, some of the broken columns did not include images or have a large margin, because we automatically broke

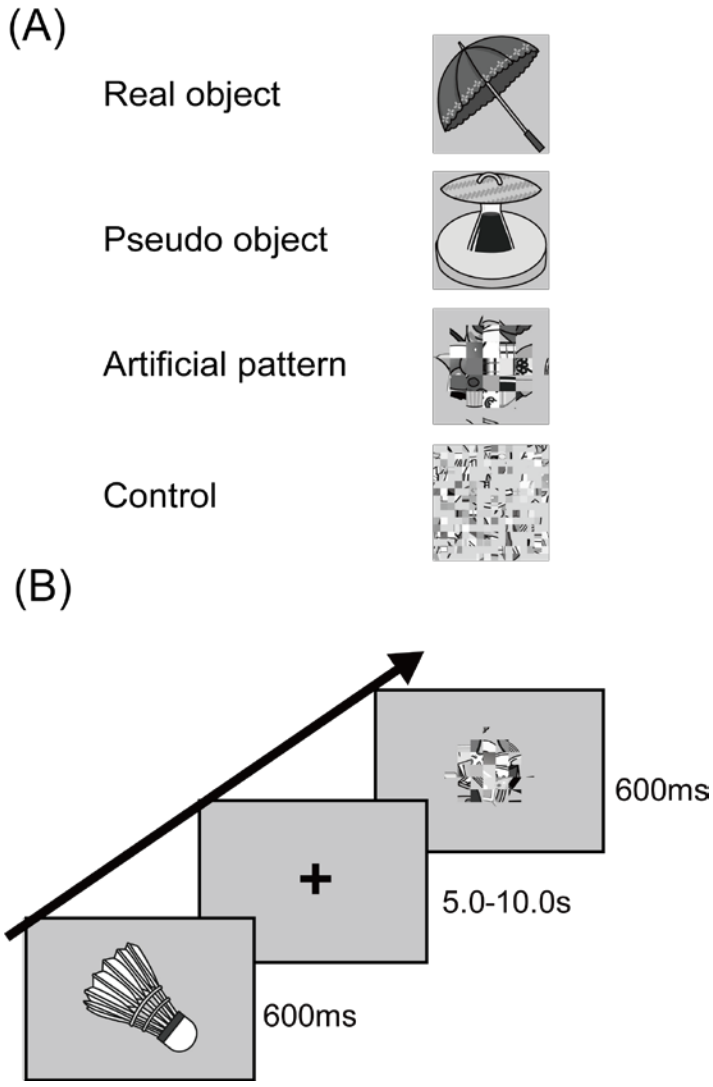

Figure 10 Stimuli examples and schematic illustration of the experimental design. (A) This figure shows four types of presented stimuli. We exposed real objects (complete structure), pseudo objects (random combinations of subcomponents), artificial patterns (fragments), and a contrast (simple photic stimuli). (B) During the fMRI session, participants were required to judge if the presented stimuli were large or small.

them into a square field which include objects, and real objects did not fill all of the square field (i.e., real objects were not square shaped). If I create artificial patterns by randomly combining these broken parts, artificial patterns may lose the unity as a whole and it looks like a contrast. To maintain the unity of the stimuli, I made artificial patterns circle shaped by semi automatically recombining these stimuli. First, real objects were automatically decomposed into 7 by 7 level and we calculated the area of the images for each broken column. Next, we filled these broken columns from the center of the square to the outside, such that columns fully containing images were arranged in the center. Contrasts were created by automatically decomposing real object characters into 16 by 16 and recomposing these components randomly. Since pseudo objects, artificial patterns, and contrasts were created by real objects, basic visual components, such as luminance, were controlled in this experiment. Full lists of stimuli can be shown in Appendix B.

2.3. Experimental Design

The experiment consisted of four fMRI sessions. Each session consisted of 20 real objects, 20 pseudo objects, 20 artificial patterns, and 20 control stimuli. Each stimulus lasted 600 ms followed by the presentation of a fixation cross (for a time period randomized from 5.0 s–10.0 s) (Figure 10B). Participants were required to judge whether the presented stimuli were large or small by pressing a button as fast and accurately as possible. All of the participants responded with the dominant hand (i.e., the right hand), but the response fingers varied across the participants, such that half of the participants responded to large stimuli using the index finger and small stimuli by

using the middle finger, and the other participants responded using the opposite stimulus/finger pattern. Prior to the experiment, participants practiced the task in the MRI scanner. The experiments were controlled by the Presentation software (Neurobehavioral Systems, Berkeley, USA). Sessions where participants failed to respond correctly to the stimuli more than 10 times were excluded from later analysis. To check how the participants responded to our tasks, the correct response rate and reaction time were analyzed by two-way repeated measures of variance (ANOVA) of stimuli type (real, pseudo, artificial, checkerboard) × size (large and small). Statistical tests were performed by R with a statistical threshold of $p < 0.01$.

2.4. fMRI data acquisition and analysis

2.4.1. fMRI acquisition

All MRI data were acquired at the National Institute of Advanced Industrial Science and Technology using a 3 Tesla Philips Ingenia scanner. For functional data acquisition, an 14-channel head coil was used (TR = 2500 ms, TE = 35 ms, flip angle = 90 °, 3.5-mm-thick axial slices, in-plane resolution = 3.12 × 3.12 mm). The first five volumes were not recorded to avoid T1 equilibration effects. Additionally, high-resolution anatomical images were obtained (slice thickness = 1.0 mm).

2.4.2. fMRI data analysis

Functional MRI data were analyzed using SPM12 (Wellcome Department of Cognitive Neurology, London, UK, http://fil.ion.ucl.ac.uk/spm/). First, slice timing was

corrected to compensate for the different acquisition time of images. These images were spatially realigned to reduce head motion. The realigned functional images were coregistered to the anatomical images. The anatomical images were segmented. Segmented tissue maps (gray matter and white matter) were used to create custom defamation fields by the DARTEL toolbox to improve spatial normalization. By using these deformation fields, functional images for participants were normalized to the MNI T1 template image. Finally, functional images were spatially smoothed with a 6 mm FWHM Gaussian filter.

Hemodynamic time series were modeled by convolving canonical hemodynamic function. The events where participants did not respond correctly were not modeled because stimuli may not be recognized. The event related evoked activation for four types of stimulus condition (real object, pseudo object, artificial pattern, and checkerboard) were modeled. These hemodynamic responses were assessed by a random-effects model that includes hypothesized hemodynamic responses of these stimulus events. A high pass filter (128 s) was applied to remove the low frequency draft of the signals.

Statistical analysis of this experiment was performed as follows. First, I illustrated differently activated brain regions across four conditions (real object, pseudo object, artificial pattern, contrast). To confirm the brain activity for each condition, Imapped brain activity for the three conditions (real object, pseudo object, and artificial pattern) in comparison to the checkerboard. The significant threshold was set at $p < 0.005$ (uncorrected), and the cluster size threshold was set at $p < 0.05$ corrected with family wise error (FWE).

2.4.3. Region of interest analysis

To compare spatial activation of object stimuli with Japanese *Kanji* characters, I defined five non-overlapping regions of interest (ROIs) which are completely identical to the first experiment. Details of this ROI analysis can be found in the methods of the first experiment; each spherical ROI had a 3 mm radius, and all of the ROIs were located along with the posterior-anterior axis (slightly declined toward the anterior direction). The center coordinates for the ROIs are as follows: (MNI coordinate [x, y, z] in mm) ROI1 (−45, −75, −12), ROI2 (−45, −67, −13), ROI3 (−45, −59, −14), ROI4 (−45, −51, −15), and ROI5 (−45, −43, −16). Likewise, ROIs in the right occipito-temporal cortex were defined in the contralateral region. The ROI definition and parameter estimate of this analysis was conducted using the MarsBaR toolbox (http://marsbar.sourceforge.net). The statistical threshold of this analysis was set at $p < 0.01$.

3. Results

3.1. Behavioral data of the size judgment task

Correct response rate of all conditions was exceeded approximately 80% (Figure 12). Correct response rate of the size judgment task was significantly different between different types (real, pseudo, artificial, or control), $F(3, 51) = 22.61$, $p < 0.001$. In contrast, I could not find difference between the object sizes (large or small) and interactive effect of size × types, $F(1, 17) = 0.14$, $p = 0.703$ and $F(3, 51) = 0.09$, $p = 0.960$ respectively. The significant difference between stimuli types could be explained by lower correct response rate for real objects. Indeed, post-hoc analysis corrected with holm revealed significant lower correct response rate of real objects in comparison to pseudo object, artificial pattern, and checkerboard, $t(17) = 4.83$, $p < 0.001$, $t(17) = 7.61$, $p < 0.001$, and $t(17) = 8.07$, $p < 0.001$ respectively. I cannot put the plausible explanation for this lower correct response rate for real objects, but I excluded incorrect events from fMRI analysis. Because participants may not attend to the stimuli satisfactory.

I found that types of stimuli (real, pseudo, artificial, or control) produced significantly different reaction times, $F(3, 51) = 26.83$, $p < 0.001$ (Figure 12). Additionally, The reaction time significantly differ between the object sizes (large or small) [$F(1, 17) = 11.76$, $p = 0.003$], such that small stimuli produced longer reaction times. However, events for small and large size stimuli were not distinguished in the fMRI analysis, because size of stimuli was not scope of this study. There was an no interactive effect of size × type on the reaction time, however, $F(3, 51) = 0.86$, $p = 0.465$.

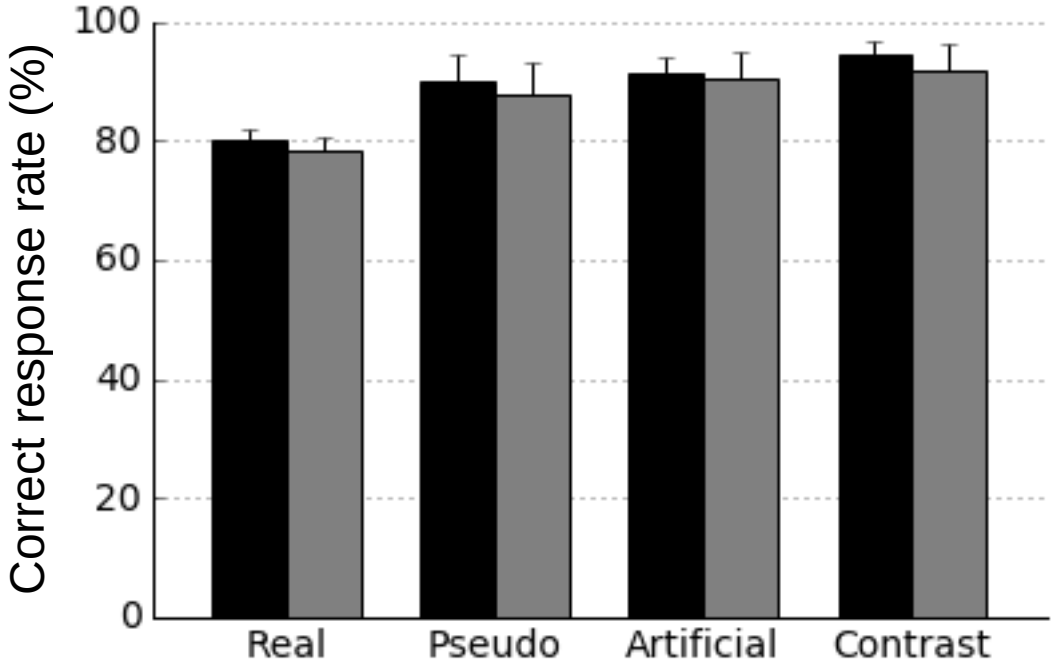

Figure 11 Correct response rate for real object, pseudo object, artificial pattern, and control stimuli. The values are the mean ± SEM (n = 18). Correct response rate for large stimuli are colored in black, and small stimuli are colored in gray.

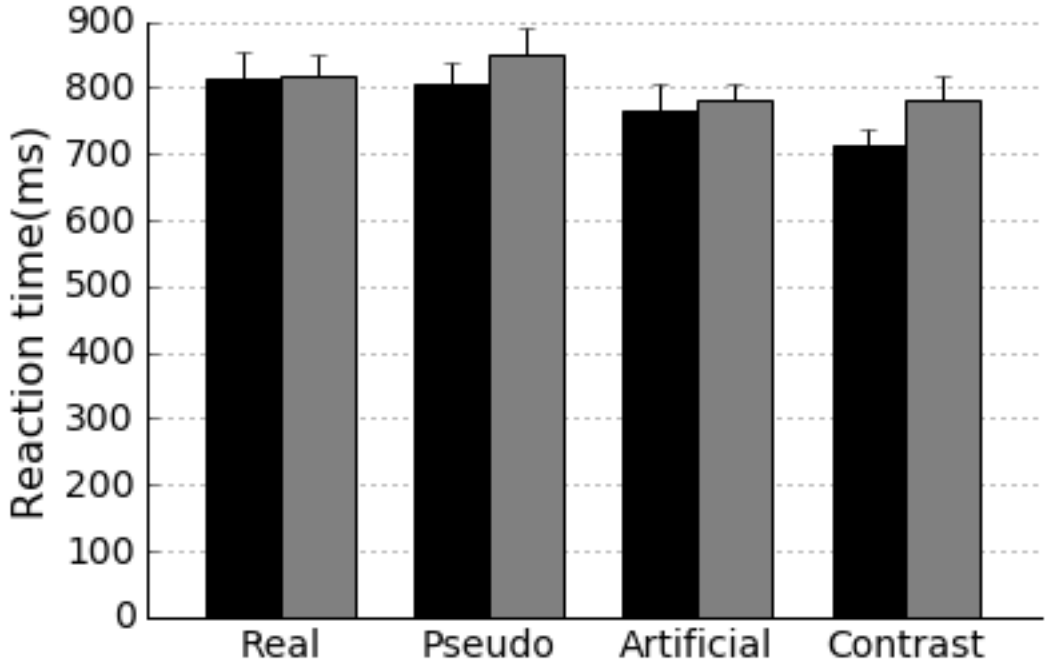

Figure 12 Response times for real object, pseudo object, artificial pattern, and control stimuli. The values are the mean ± SEM (n = 18). Response times for large stimuli are colored in black, and small stimuli are colored in gray.

3.2. fMRI data

3.2.1. Differently activated brain region among all types of Object stimuli

To identify how different object stimuli produced brain activity, we compared four activation maps (real object, pseudo object, artificial pattern, and control) and illustrated differently activated brain regions (Figure 13 and Table 4). The bilateral occipito-temporal inferior temporal gyri, bilateral fusiform gyri, right precentral gyrus, and right inferior frontal gyrus were differently activated by these stimuli. I could confirm that the four types of condition we presented differently activated the ventral visual pathway, including the bilateral fusiform gyri and the bilateral occipital cortices.

3.2.2. Brain activations for each types of Object stimuli

For further investigation of brain activation for each type of object stimuli, I mapped brain activity for real objects, pseudo objects, and artificial patterns in comparison to control stimuli (Figure 14 and Table 5). The real object activated widespread brain regions such as the bilateral inferior and the middle frontal gyri, and the bilateral occipito-temporal cortex including left inferior temporal gyrus, left occipital fusiform gyrus, left inferior occipital gyrus, and right fusiform gyrus . Cluster size for the left occipito-temporal cortex is larger than right occipito-temporal cortex. Cluster of the left occipito-temporal cortex was extended to the superior parietal lobule, however brain activity of this brain region was weak and central part of activation was occipito-temporal cortex. Likewise, the pseudo object produced brain activity in the bilateral occipito-temporal cortices including the bilateral fusiform and lingual gyri. Aside from real object, pseudo object did not produced brain activity in the middle and

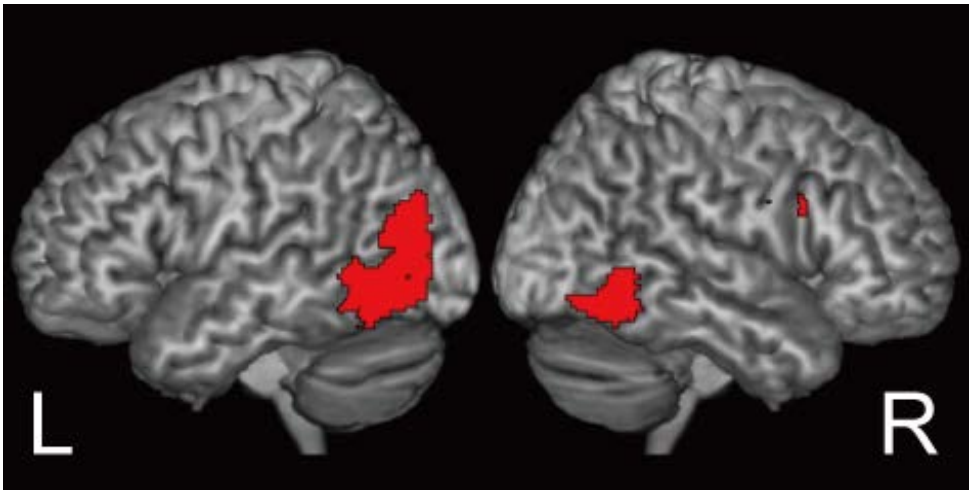

Figure 13 Brain activation maps of differently activated brain regions due to real objects, pseudo objects, artificial patterns, and contrasts. The bilateral occipito-temporal cortices were differently activated by these stimuli. The height threshold of this analysis was $p < 0.005$, with a cluster wise threshold $p < 0.05$ (family wise error corrected).

Table 4 Differently activated brain regions in response to real objects, pseudo objects, artificial patterns, and a control.

Region	MNI Coordinates (mm)			F	voxels
	x	y	z		
L Inferior Occipital Gyrus	-38	-68	-10	14.56	1738
L Inferior Temporal Gyrus	-46	-60	-10	12.27	
L Fusiform Gyrus	-42	-80	18	11.84	
R Inferior Temporal Gyrus	52	-60	-8	12.51	598
R Fusiform Gyrus	44	-56	-16	9.08	
R Middle Temporal Gyrus	58	-54	-2	8.47	
R Precentral Gyrus	38	2	24	8.43	274
R Inferior Frontal Gyrus	28	4	20	7.64	
R Inferior Frontal Gyrus	40	14	18	7.51	

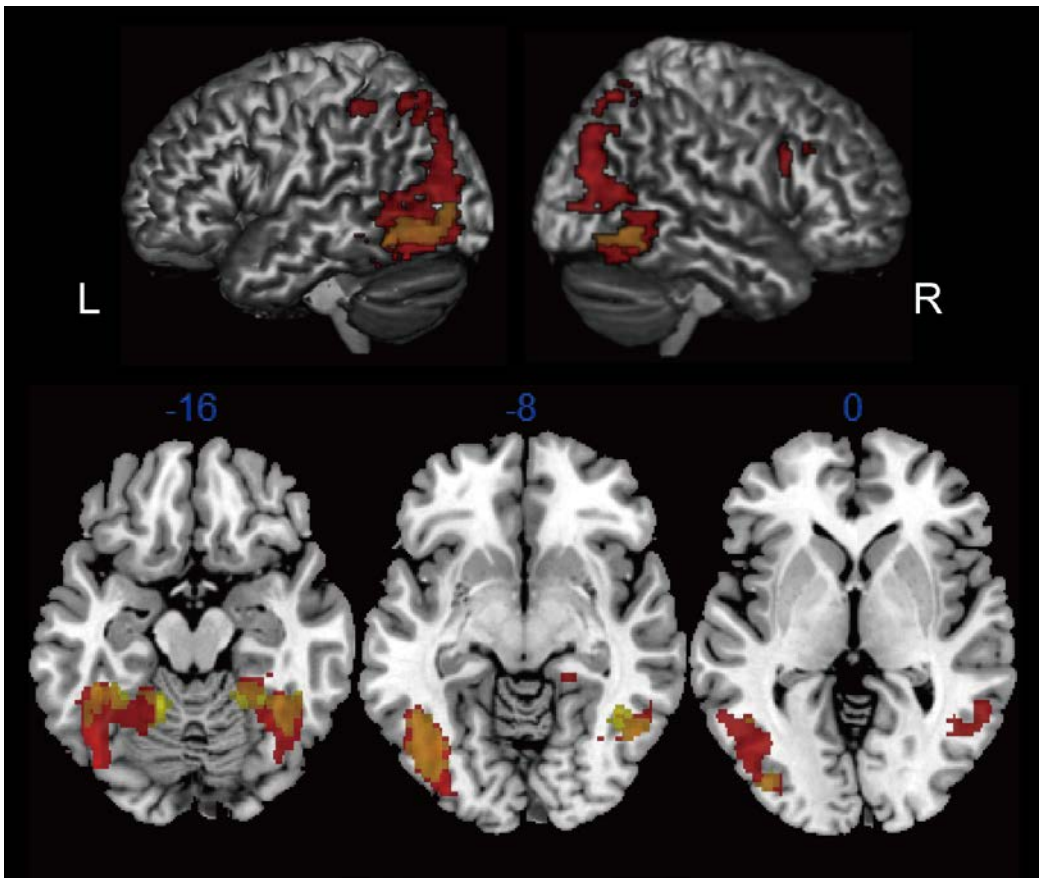

Figure 14 Activated brain regions for real and pseudo objects in comparison with a control. The height threshold was set at $p < 0.005$ with a cluster level threshold $p < 0.05$ (FWE corrected). The brain activity for real objects are colored in red and the pseudo objects are colored in yellow. The artificial pattern did not produce brain activity using this statistical threshold. I found the real and pseudo objects significantly activated the bilateral occipito-temporal cortices.

Table 5 Brain activity produced by real and pseudo objects.

Region	MNI Coordinates (mm)			T	voxels
	x	y	z		
Real > Control					
L Inferior Temporal Gyrus	-48	-58	-12	6.52	3905
L Occipital Fusiform Gyrus	-36	-70	-10	6.32	
L Inferior Occipital Gyrus	-36	-82	-6	5.62	
R Inferior Frontal Gyrus	40	16	18	6.03	329
R Middle Frontal Gyrus	34	20	32	4.60	
R Inferior Frontal Gyrus	42	14	26	3.89	
R Middle Occipital Gyrus	34	-80	20	5.52	1009
R Middle Occipital Gyrus	32	-78	28	5.16	
R Precuneus	18	-72	40	5.09	
R Superior Frontal Gyrus	18	-12	34	5.41	465
R Superior Frontal Gyrus	14	30	36	5.21	
R Anterior Cingurate Gyrus	4	24	30	5.09	
R Fusiform Gyrus	38	-48	-16	5.08	1090
R Fusiform Gyrus	34	-58	-18	4.96	
R Fusiform Gyrus	24	-44	-20	4.82	

Pseudo > Control					
R Fusiform Gyrus	28	-44	-24	5.86	617
R Inferior Temporal Gyrus	42	-54	-8	4.71	
R Lingual Gyrus	48	-44	-16	3.8	
L Lingual Gyrus	-14	-50	-14	5.76	885
L Fusiform Gyrus	-28	-48	-20	5.34	
L Fusiform Gyrus	-40	-42	-14	5.17	

inferior frontal gyrus. However, I failed to find brain activity for the artificial pattern in the statistical threshold I applied. I was able to confirm the real and pseudo object significantly activated the bilateral occipito-temporal cortices.

3.2.3. Different spatial patterns of activation within the left occipito-temporal cortex for three types of stimuli

To examine how each type of object stimuli induced a spatial distribution pattern within the bilateral occipito-temporal cortices, I created consecutive ROIs within the bilateral occipito-temporal cortices and compared the spatial distribution patterns (Figure 15). The created ROIs were the same as that of the *Kanji* experiment (Experiment 1). Three-way repeated measures ANOVA of contrast estimate reveals main effect of ROI locations and stimulus types, $F(4,64) = 3.842$, $p = 0.007$, $F(2,32) = 6.158$, $p = 0.005$ respectively. Contrary to the *Kanji* experiment, main effect of laterality (left, and right hemisphere) did not reach significant level, $F(1,16) = 0.398$, $p = 0.536$. To investigate spatial distribution pattern within the occipito-temporal cortex, I investigated interactive effect between ROIs and stimuli types. In the left occipito-temporal cortex, two-way repeated measures ANOVA of the contrast estimate of activations did not revealed an interactive effect of ROI locations × character types. Three types of stimuli showed similar activation patterns, such that the brain activation patterns were decreased along the posterior-anterior axis. In contrast, the right occipito-temporal cortex produced significant interactive effect of ROI locations (1–5) × object types (real, pseudo, and artificial), $F(8,120) = 4.168$, $p = 0.0002$. This interaction seems contradictory to the result of three-way repeated measures ANOVA, although this

interactive effect can be explained by the different activation pattern in response to real and pseudo objects versus artificial patterns. Real and pseudo objects exhibited decreased brain activity along the posterior to anterior axis. However, artificial characters showed almost the same brain activity across ROIs. In contrast with result of *Kanji* character, real and pseudo objects showed similar activation pattern within the bilateral occipito-temporal cortex.

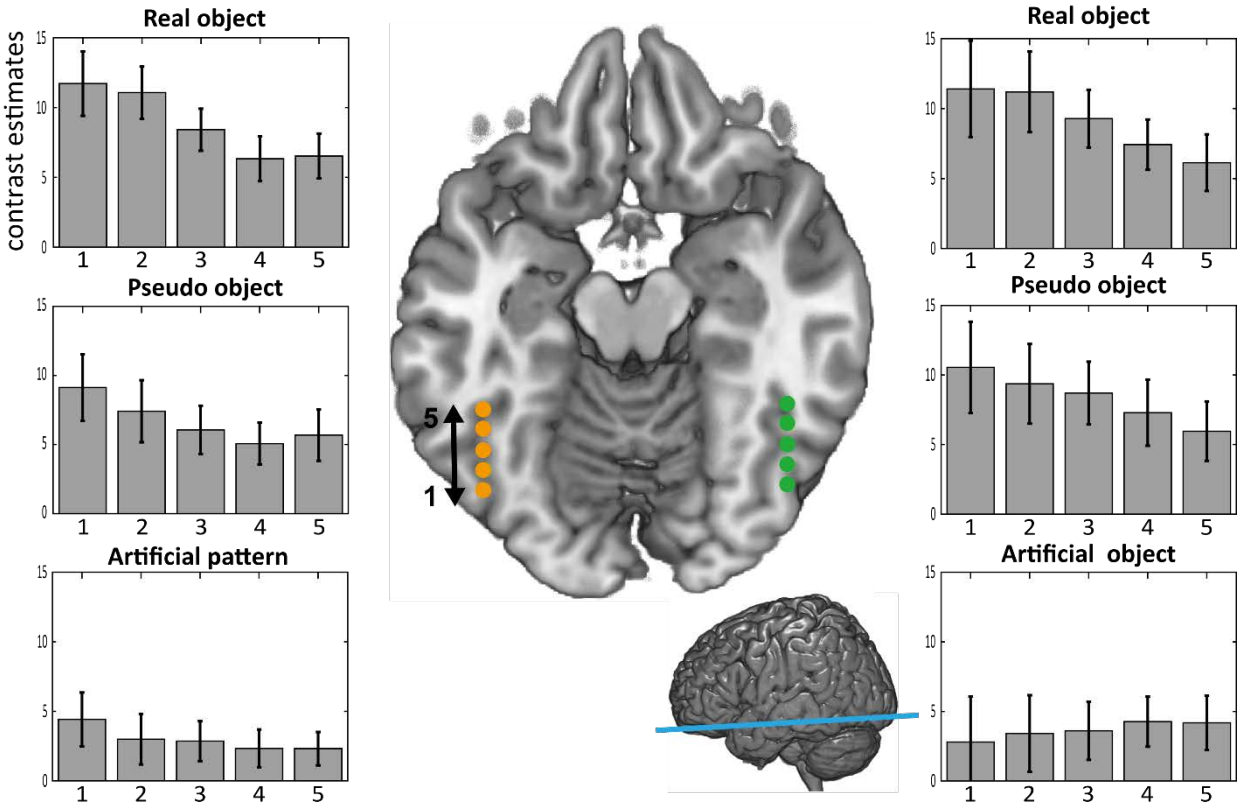

Figure 15 ROI analysis for each kind of stimuli in bilateral occipito-temporal cortices. ROIs were aligned with posterior to anterior axis. The ROI numbered in 1 (ROI1) is most posterior ROI and ROI numbered in 5 (ROI5) is a most anterior ROI. The bar graphs show the contrast estimate (a.u.) of brain activity within each ROIs. The error bars represent standard errors across participants. Orange and green circle shows ROIs for left and right occipito-temporal cortex, respectively.

4. Discussion

The purpose of this experiment was to investigate how objects are recognized hierarchically in the bilateral occipito-temporal cortices. We first confirmed four types of stimuli (real object, pseudo object, artificial pattern, and control stimuli) differently activate the bilateral occipito-temporal cortices. This difference can be explained by distinct activation patterns between real and pseudo object stimuli vs. artificial pattern stimuli. When brain activities were compared with the activity in response to a control stimuli, real and pseudo objects produced a similar activation patterns, although I failed to find significant brain activity for artificial patterns using the statistical threshold of this experiment. The ROI analysis confirmed a similar activation pattern among objects stimuli in the left occipito-temporal cortex. The interactive effect of ROIs × stimuli types was found in the right occipito-temporal cortex. However, this interactive effect can be explained by the different activation pattern in response to real and pseudo objects versus artificial patterns.

The brain activation for objects has been investigated in many studies. Some researchers implied domain-specific representation in the occipito-temporal cortices, such that there is a specialized brain area for faces, places, body parts, and objects (Kanwisher, McDermott, and Chun 1997; Downing et al. 2001; Grill-Spector, Sayres, & Ress, 2006). In this experiment, I did not include the human face, places, or human body parts as real object stimuli as shown in appendix B. Thus, an object recognition system might be recruited in this experiment. Indeed, our results were consistent with previous studies that compared brain activity for the face, place, body parts, and

objects(Spiridon, Fischl, & Kanwisher, 2006). The peak location of real objects in the right fusiform gyrus (x = 38, y = −48, z = −16) was just 9.29 mm apart from the peak location of the object which has been defined in a previous study (x = 28.8, y = −49.2, z = −16.5). Likewise, peak location in the left inferior temporal gyrus (x = −48, y = −58, z = −12) was quite close to the previously reported peak loci (x = −45.8, y = −53.7, z = −11.5) (~5 mm apart). I cannot conclude that objects are recognized in a domain-specific manner, because I did not compare brain activity between different categories (i.e., human face, places, body parts, and objects). However, the experiment was successful in the measurement of brain activity within the visual object recognition system.

I found similar brain activity between real and pseudo objects, such that occipito-temporal brain activity for both stimuli were stronger in the posterior ROIs compared with brain activity in the anterior ROIs. Why did real and pseudo objects produce a similar activation pattern? The cortical column, which is a basic computational unit in the cortex, might be able to explain this similar activation pattern. There are columns for visual features of objects in the anterior inferotemporal area in monkeys (Fujita, Tanaka, Ito, & Cheng, 1992). Another study showed complex objects are represented by the combination of feature columns, such that representation of mugs consist of the body and handle (Tsunoda, Yamane, Nishizaki, & Tanifuji, 2001). Spatial resolution of non-invasive neuroimaging techniques limits direct investigation of the column structure in humans, although some studies imply the existence of a column structure in the human occipito-temporal cortex (e.g., Grill-Spector et al. 2006). I made pseudo objects by recomposing parts of objects. Thus, the same columns might be

activated between real and pseudo objects as a whole, resulting in similar activation patterns between these stimuli. However, this idea is still speculative and warrants investigation in future studies.

Another finding of this experiment is that I could not find significant brain activity for artificial patterns, which probably leads to the observed difference between real and pseudo objects versus artificial patterns. Artificial patterns were made by automatically decomposing real objects into a 7 by 7 level and randomly recomposing these images. A previous study, which compared brain activity in response to photos and scrambled photos, showed that photos decomposed 8 × 8 produced decreased brain activity in the lateral occipital cortex compared with photos decomposed 4 × 4 (Grill-Spector et al., 1998). These scrambled photos are quite similar to our artificial patterns, although our artificial patterns contain fragments of objects. Previous results and our present results imply highly decomposed objects decrease brain activity in comparison to real objects. The second possibility of this weak brain activity for artificial patterns is the stimulus presentation time. In this experiment, stimuli were exposed quite quickly (600 ms), and participants may fail to recognize fragment of objects, because fragments of objects are quite small and seem to be difficult to recognize.

In summary, I found similar brain activity due to real and pseudo objects when compared with a control; this may be explained by the distributed representation of objects. Conversely, I could not find significant different brain activity for artificial patterns compared to the brain activity observed with a control.

Chapter V General discussion

The purpose of this study was to investigate how the visual character forms of Japanese *Kanji* are processed in the brain. Studies in alphabetic script showed visual word forms are processed hierarchically in the left occipito-temporal cortex (Dehaene et al. 2005; Vinckier et al. 2007). Japanese *Kanji* characters consist of hierarchical components, such as strokes, radicals, and characters. I hypothesized hierarchical visual components of Japanese *Kanji* characters activate different brain regions within the left occipito-temporal cortex. As I expected, brain activations were aligned from posterior to anterior hierarchically within the left occipito-temporal cortex, such that pseudo *Kanji*, which include radicals, activated the more posterior part of the brain compared with real *Kanji* characters. However, I could not found this spatial distribution pattern in the experiment for objects.

As I went over in my discussion of the first experiment, the novelty of pseudo *Kanji* characters may have some influence on character form processing with the left occipito-temporal cortex. Some previous studies claimed that the novelty of visual stimuli changes brain activity in the occipito-temporal cortices (Xiang & Brown, 1998; Zhang et al., 2013). However, I think that different spatial distribution patterns of the brain activity in response to real, pseudo, and artificial characters cannot simply account for the novelty of the visual stimuli for the following reasons. First, the peak activation region for artificial characters was more posterior than that of the pseudo *Kanji* character. Pseudo *Kanji* characters were made by exchanging radicals. Hence, pseudo *Kanji* characters look like *Kanji* characters, although not as whole characters. In contrast,

artificial characters were decomposed into the stroke level and then we recombined these components, resulting in artificial characters that are completely novel visual stimuli. If the differential spatial distribution pattern is driven by the novelty of visual stimuli, artificial characters should activate distinct or more anterior brain regions compared with pseudo and real *Kanji* characters. However, most activated brain regions for artificial character were more posterior than that in response to real and pseudo *Kanji* characters in the experiment 2. Second, I did not find different spatial distribution patterns between real and pseudo objects. Because pseudo objects are a manmade stimulus, pseudo objects are more novel than real objects. If the different spatial distribution pattern for *Kanji* characters is induced by the novelty of visual stimuli, real and pseudo objects should produce different spatial distribution patterns. Thus, it is reasonable to think that hierarchical character form processing of Japanese *Kanji* characters is not produced by novelty of visual stimuli.

How are the visual forms of Japanese *Kanji* characters represented within the occipito-temporal cortices? Because fMRI signals are thought to represent averaged neural activity within voxels, I cannot directly assess the neural representation of Japanese *Kanji* characters. However, the current experiments provide a clue to understand this representation. In the first experiment, I found significant interaction between ROI and stimulus types (i.e., real *Kanji*, pseudo *Kanji*, and artificial character) in the left occipito-temporal cortex, but this interaction was not found in the right occipito-temporal cortex. A similar result was found in an experiment on alphabetic "words" (Vinckier et al., 2007). In this previous study, subjects were exposed to strings of false fonts, infrequent letters, frequent letters, frequent bigrams, frequent quadrigrams,

and words to examine the spatial organization pattern within the occipito-temporal cortex. As in my experiment, they created ROIs along the posterior to anterior axis within the bilateral occipito-temporal cortex and calculated the brain activity for each ROI. Consistent with the findings of the current study, they found strong interaction between ROIs and stimulus types only in the left occipito-temporal cortex. Additionally, the ROI ($x = -48$, $y = -55$, $z = -16$), which is close to the VWFA of the alphabetic script, shows stronger brain activity for words in comparison to other types of stimuli (e.g., bigrams, and letters). This particular ROI is very close to ROI3 ($x = -45$, $y = -59$ $z = -13$) of my experiment, which exhibits the largest amount of brain activity for Japanese *Kanji* characters. In contrast, the more posterior ROI ($x = -45$, $y = -70$ $z = -12$) is shown to produce uniform activation patterns across stimuli. This ROI is also close to the posterior ROI in my experiment, and peak activation of artificial character has been recorded in this ROI. Based on the findings of the current study, it has been postulated that visual forms of Japanese *Kanji* characters could be recognized as alphabetic words.

As discussed in the second experiment, real and pseudo objects produced similar activation patterns, which may reflect columns representation of object representation. When I consider the visual word and character form system was developed to be good at visual system, visual word and character form processing may have a similar neural representation pattern to the object recognition system. This leads to the possibility that there might be column for radicals the combination of which represent Japanese *Kanji* character. This idea seems to conflict with my results because real and pseudo *Kanji* character produced different spatial distribution pattern. However, real *Kanji* characters are pronounceable and contain semantic information, and pseudo

Kanji characters do not provide semantic information. The language specific factor such as semantic and phonological information of real *Kanji* characters may contribute to the hierarchical spatial distribution pattern for *Kanji* characters.

In summary, my two experiments may be explained as follows. Basically, visual forms of objects and *Kanji* characters are processed hierarchically within the occipito-temporal cortex, such that fragments and subcomponents (i.e., radicals and object parts) are processed from posterior to anterior regions. However, visual forms of whole objects and *Kanji* characters themselves may be represented as combinations of subcomponents as I discussed in the previous paragraph. For *Kanji* characters, representation of visual character forms is conveyed to the anterior brain region and language-specific processing such as semantic and/or phonological may be conducted independently. However, this idea needs to be interpreted with caution because our experiment did not directly investigate the neural representation of *Kanji* characters and objects. This idea should be investigated in future studies.

I found that visual character forms of Japanese *Kanji* characters were hierarchically recognized in the left occipito-temporal cortex. On the other hands, this hierarchical spatial distribution pattern was not found for objects. These results imply that the hierarchical spatial distribution pattern for Japanese *Kanji* characters might be induced by language-specific cognitive components. In this study, I did not examine the hierarchical spatial distribution pattern of Japanese *Kana* words. Investigating visual word form processing of *Kana* words might contribute to understanding regarding which components of language contribute to hierarchical processing because *Kana* letters do not have semantic information. Future studies are needed to examine the

hierarchical coding of visual forms for Japanese *Kanji* and *Kana* characters.

Acknowledgment

I would like to thank Dr. Akira Uno at University of Tsukuba for his contentious support. I am also grateful to Dr. Yoshiya Moriguchi at Lundbeck Japan for lending his expertise of MRI experiment and useful discussion. Finally, I wish to thank Dr. Sunao Iwaki at national institute of advanced industrial science and technology for supporting my experiment.

References

Allport, D. A. (1977). On knowing the meaning of words we are unable to report: The effects of visual masking. In S. Dornic (Ed.), *Attention and performance VI* (pp. 505–533). Hillsdale, NJ: Erlbaum.

Amano, S., & Kondo, K. (2003). *NTT Psycholinguistic Database*. Sansedo, Tokyo.

Anzai, A., Peng, X., & Van Essen, D. C. (2007). Neurons in monkey visual area V2 encode combinations of orientations. *Nature Neuroscience*, *10*(10), 1313–1321.

Arguin, M., & Bub, D. N. (1993). Single-character processing in a case of pure alexia. *Neuropsychologia*, *31*(5), 435–458.

Baylis, G. C., Rolls, E. T., & Leonard, C. M. (1987). Functional subdivisions of the temporal lobe neocortex. *The Journal of Neuroscience*, *7*(2), 330–42.

Behrmann, M., Nelson, J., & Sekuler, E. . (1998). Visual complexity in letter-by-letter reading: Pure alexia is not pure. *Neuropsychologia*, *36*(11), 1115–1132.

Beversdorf, D., Stommel, E., Allen, C. n, Stevens, R., & Lessell, S. (1997). Recurrent branch retinal infarcts in association with migraine. *Headache: The Journal of Head and Face Pain*, *37*(6), 396–399.

Binder, J. R., & Mohr, J. P. (1992). The topography of callosal reading pathways. A case-control analysis. *Brain*, (6), 1807–26.

Bolger, D. J., Perfetti, C. A., & Schneider, W. (2005). Cross-cultural effect on the brain revisited: universal structures plus writing system variation. *Human Brain Mapping*, *25*(1), 92–104.

Brincat, S. L., & Connor, C. E. (2004). Underlying principles of visual shape selectivity

in posterior inferotemporal cortex. *Nature Neuroscience, 7*(8), 880–886.

Brunswick, N., McCrory, E., Price, C. J., Frith, C. D., & Frith, U. (1999). Explicit and implicit processing of words and pseudowords by adult developmental dyslexics: A search for Wernicke's Wortschatz? *Brain*, (10), 1901–17.

Chan, S., Tang, S., Tang, K., Lee, W., Lo, S., & Kwong, K. K. (2009). Hierarchical coding of characters in the ventral and dorsal visual streams of Chinese language processing. *Neuroimage*, *48*(2), 423–435.

Chen, M. J., & Yung, Y. F. (1989). Reading Chinese: A holistic or piecemeal process? In A. F. Bennet & K. J. McConkey, (Eds.), *Cognition in individual and social context* (pp. 91–100). Amsterdam: Elsevier.

Cohen, L., Dehaene, S., Naccache, L., Lehericy, S., Dehaene-Lambertz, G., Henaff, M. A., … Michel, F. (2000). The visual word form area: spatial and temporal characterization of an initial stage of reading in normal subjects and posterior split-brain patients. *Brain*, *123*(2), 291–307.

Cohen, L., Lehéricy, S., Chochon, F., Lemer, C., Rivaud, S., & Dehaene, S. (2002). Language-specific tuning of visual cortex? Functional properties of the Visual Word Form Area. *Brain*, *125*(5), 1054–1069.

Coltheart, M., Rastle, K., Perry, C., Langdon, R., & Ziegler, J. (2001). DRC: A Dual Route Cascaded Model of visual word recognition and reading aloud. *Psychological Review*, *108*(1), 204–56.

Damasio, A. R., & Damasio, H. (1983). The anatomic basis of pure alexia. *Neurology*, *33*(12), 1573–1573.

Dehaene, S., & Cohen, L. (2007). Cultural recycling of cortical maps. *Neuron*, *56*(2),

384–398.

Dehaene, S., Cohen, L., Sigman, M., & Vinckier, F. (2005). The neural code for written words: a proposal. *Trends in Cognitive Sciences*, *9*(7), 335–341.

Dehaene, S., Pegado, F., Braga, L. W., Ventura, P., Nunes Filho, G., Jobert, A., … Cohen, L. (2010). How learning to read changes the cortical networks for vision and language. *Science*, *330*(6009), 1359–1364.

Dejerine, J. J. (1891). Sur un cas de cécité verbale avec agraphie suivi d'autopsie. *Mémoires de La Société de Biologie*, *3*, 197–201.

Dejerine, J. J. (1892). Contribution a l'étude anatomo-pathologique et clinique des différentes variétés de cécité verbale. *Universitätsbibliothek Johann Christian Senckenberg*, *44*(9. ser. tom. 4), 61–90.

Dietz, N. A. E., Jones, K. M., Gareau, L., Zeffiro, T. A., & Eden, G. F. (2005). Phonological decoding involves left posterior fusiform gyrus. *Human Brain Mapping*, *26*(2), 81–93.

Ding, G., Peng, D., & Taft, M. (2004). The nature of the mental representation of radicals in Chinese: A priming study. *Journal of Experimental Psychology: Learning Memory and Cognition*, *30*(2), 530–539.

Downing, P. E., Jiang, Y., Shuman, M., & Kanwisher, N. (2001). A cortical area selective for visual processing of the human body. *Science*, *293*(5539), 2470–2473.

Fang, S., & Wu, P. (1989). Illusory conjunctions in the perception of Chinese characters. *Journal of Experimental Psychology: Human Perception and Performance*, *15*(3), 434–447.

Felleman, D. J., & Van Essen, D. C. (1991). Distributed hierarchical processing in the

primate cerebral cortex. *Cerebral Cortex*, *1*(1), 1–47.

Flechsig, P. (1901). Developmental (myelogenetic) localisation of the cerebral cortex in the human subject. *The Lancet*, *158*(4077), 1027–1030.

Flores d'Arcais, G. B., Saito, H., & Kawakami, M. (1995). Phonological and semantic activation in reading kanji characters. *Journal of Experimental Psychology: Learning, Memory, and Cognition*, *21*(1), 34–42.

Fujita, I., Tanaka, K., Ito, M., & Cheng, K. (1992). Columns for visual features of objects in monkey inferotemporal cortex. *Nature*, *360*(6402), 343–346.

Geschwind, N. (1965). Disconnexion syndromes in animals and man. I. *Brain*, *88*(2), 237–94.

Grainger, J., Dufau, S., Montant, M., Ziegler, J. C., & Fagot, J. (2012). Orthographic processing in Baboons (Papio papio). *Science*, *336*(6078), 245–248.

Grill-Spector, K., Kushnir, T., Hendler, T., Edelman, S., Itzchak, Y., & Malach, R. (1998). A sequence of object-processing stages revealed by fMRI in the human occipital lobe. *Human Brain Mapping*, *6*(4), 316–328.

Grill-Spector, K., Sayres, R., & Ress, D. (2006). High-resolution imaging reveals highly selective nonface clusters in the fusiform face area. *Nature Neuroscience*, *9*(9), 1177–1185.

Han, B. (1994). Frequency effect of constituent in Chinese character recognition. In Q. Jing, H. Zhang, & D. Peng (Eds.), *Information processing of the Chinese language* (pp. 87–98). Beijing: Beijing Normal Univ. Press.

Hegdé, J., & Van Essen, D. C. (2000). Selectivity for complex shapes in primate visual area V2. *The Journal of Neuroscience*, *20*(5), 61–66.

Henson, R., & Friston, K. (2007). Convolution models for fMRI. In K. J. Friston, J. Ashburner, S. Kiebel, T. Nichols, & W. D. Penny (Eds.), *Statistical Parametric Mapping* (2nd ed., pp. 178–192). London: Elsevier/Academic Press.

Hoeft, F., Meyler, A., Hernandez, A., Juel, C., Taylor-Hill, H., Martindale, J. L., … Gabrieli, J. D. E. (2007). Functional and morphometric brain dissociation between dyslexia and reading ability. *Proceedings of the National Academy of Sciences of the United States of America*, *104*(10), 4234–4239.

Hubel, D. H., & Wiesel, T. N. (1962). Receptive fields, binocular interaction and functional architecture in the cat's visual cortex. *The Journal of Physiology*, *160*(1), 106–154.

Ito, M., & Komatsu, H. (2004). Representation of angles embedded within contour stimuli in area V2 of macaque monkeys. *Journal of Neuroscience*, *24*(13), 3313–3324.

Iwata, M. (1984). Kanji versus Kananeuropsychological correlates of the Japanese writing system. *Trends in Neurosciences*, *7*(8), 290–293.

Kanwisher, N., McDermott, J., & Chun, M. M. (1997). The fusiform face area: a module in human extrastriate cortex specialized for face perception. *Journal of Neuroscience*, *17*(11), 4302–4311.

Kobatake, E., & Tanaka, K. (1994). Neuronal selectivities to complex object features in the ventral visual pathway of the macaque cerebral cortex. *Journal of Neurophysiology*, *71*(3), 856–867.

Kuo, W. J., Yeh, T. C., Lee, J. R., Chen, L. F., Lee, P. L., Chen, S. S., … Hsieh, J. C. (2004). Orthographic and phonological processing of Chinese characters: an fMRI

study. *NeuroImage*, *21*(4), 1721–1731.

Kwon, J. C., Lee, H. J., Chin, J., Lee, Y. M., Kim, H., & Na, D. L. (2002). Hanja alexia with agraphic after left posterior inferior temporal lobe infarction: A case study. *Journal of Korean Medical Science*, *17*(1), 91–95.

Lai, C., & Huang, J. T. (1988). Component migration in Chinese characters: Effects of priming and context on illusory conjunction. In I. M. Liu, H. C. Chen, & Chen M.J. (Eds.), *Cognitive aspects of the Chinese language* (pp. 57–67). Hong Kong: Asian Research Service.

Leong, C. K., Cheng, P.-W., & Mulcahy, R. (1987). Automatic processing of morphemic orthography by mature readers. *Language and Speech*, *30*(2), 181–196.

Liu, C., Zhang, W. T., Tang, Y. Y., Mai, X. Q., Chen, H. C., Tardif, T., & Luo, Y. J. (2008). The Visual Word Form Area: Evidence from an fMRI study of implicit processing of Chinese characters. *NeuroImage*, *40*(3), 1350–1361.

Malonek, D., Dirnagl, U., Lindauer, U., Yamada, K., Kanno, I., & Grinvald, A. (1997). Vascular imprints of neuronal activity: relationships between the dynamics of cortical blood flow, oxygenation, and volume changes following sensory stimulation. *Proceedings of the National Academy of Sciences of the United States of America*, *94*(26), 14826–31.

McClelland, J. L., & Rumelhart, D. E. (1981). An interactive activation model of context effects in letter perception: I. An account of basic findings. *Psychological Review*, *88*(5), 375–407.

Michael, A. S., Indra, K., Bent, M., Gesa, S., Nicole, E. N., Jens, B., … Angela, D. F. (2016). NRSN1 associated grey matter volume of the visual word form area

reveals dyslexia before school. *Brain*, *33*(27), 11296–11301.

Nakamura, K., Oga, T., Okada, T., Sadato, N., Takayama, Y., Wydell, T., … Fukuyama, H. (2005). Hemispheric asymmetry emerges at distinct parts of the occipitotemporal cortex for objects, logograms and phonograms: a functional MRI study. *Neuroimage*, *28*(3), 521–528.

Oldfield, R. C. (1971). The assessment and analysis of handedness: the Edinburgh inventory. *Neuropsychologia*, *9*(1), 97–113.

Paulesu, E., Démonet, J. F., Fazio, F., McCrory, E., Chanoine, V., Brunswick, N., … Frith, U. (2001). Dyslexia: cultural diversity and biological unity. *Science*, *291*(5511), 2165–7.

Paulesu, E., Frith, U., Snowling, M., Gallagher, A., Morton, J., Frackowiak, R. S., & Frith, C. D. (1996). Is developmental dyslexia a disconnection syndrome? Evidence from PET scanning. *Brain*, (1), 143–57.

Peng, D. L., Li, Y. P., & Yang, H. (1997). Orthographic processing in the identification of Chinese characters. In H.-C. Chen (Ed.), *Cognitive processing of Chinese and related Asian languages* (pp. 85–108). Hong Kong: The Chinese University Press.

Perry, C., Ziegler, J. C., & Zorzi, M. (2007). Nested incremental modeling in the development of computational theories: the CDP+ model of reading aloud. *Psychological Review*, *114*(2), 273–315.

Pugh, K. R., Mencl, W. E. E., Jenner, A. R., Katz, L., Frost, S. J., Lee, J. R., … Shaywitz, B. A. (2001). Neurobiological studies of reading and reading disability. *Journal of Communication Disorders*, *34*(6), 479–492.

Richlan, F., Kronbichler, M., & Wimmer, H. (2009). Functional abnormalities in the

dyslexic brain: A quantitative meta-analysis of neuroimaging studies. *Human Brain Mapping*, *30*(10), 3299–3308.

Rumelhart, D. E., & McClelland, J. L. (1982). An interactive activation model of context effects in letter perception: II. The contextual enhancement effect and some tests and extensions of the model. *Psychological Review*, *89*(1), 60–94.

Rumsey., J. M., Andreason., P., Zametkin., A. J., Aquino., T., King., A. C., Hamburge., S. D., … Cohen., R. M. (1992). Failure to activate the left temporoparietal cortex in dyslexia. *Archives of Neurology*, *49*(5), 527–534.

Saito, H., Masuda, H., & Kawakami, M. (1999). Subword activation in reading Japanese single Kanji character words. *Brain and Language*, *68*(1), 75–81.

Salmelin, R., Kiesilä, P., Uutela, K., Service, E., & Salonen, O. (1996). Impaired visual word processing in dyslexia revealed with magnetoencephalography. *Annals of Neurology*, *40*(2), 157–162.

Schmolesky, M. T., Wang, Y., Hanes, D. P., Thompson, K. G., Leutgeb, S., Schall, J. D., & Leventhal, A. G. (1998). Signal timing across the macaque visual system. *Journal of Neurophysiology*, *79*(6), 3272–8.

Shallice, T., & McGill, J. (1978). The origins of mixed errors. In J. Requin (Ed.), *Attention and performance VII* (pp. 193–208). Hillsdale, NJ: Erlbaum.

Shaywitz, B. A., Shaywitz, S. E., Pugh, K. R., Mencl, W. E. E., Fulbright, R. K., Skudlarski, P., … Gore, J. C. (2002). Disruption of posterior brain systems for reading in children with developmental dyslexia. *Biological Psychiatry*, *52*(2), 101–110.

Shaywitz, S. E., Shaywitz, B. A., Pugh, K. R., Fulbright, R. K., Constable, R. T., Mencl,

W. E., … Gore, J. C. (1998). Functional disruption in the organization of the brain for reading in dyslexia. *Proceedings of the National Academy of Sciences of the United States of America*, *95*(5), 2636–2641.

Simos, P. G., Breier, J. I., Fletcher, J. M., Foorman, B. R., Bergman, E., Fishbeck, K., & Papanicolaou, A. C. (2000). Brain activation profiles in dyslexic children during non-word reading: a magnetic source imaging study. *Neuroscience Letters*, *290*(1), 61–65.

Spiridon, M., Fischl, B., & Kanwisher, N. (2006). Location and spatial profile of category-specific regions in human extrastriate cortex. *Human Brain Mapping*, *27*(1), 77–89.

Su, I. F., Mak, S. C., Cheung, L. M., & Law, S. (2012). Taking a radical position: evidence for position-specific radical representations in Chinese character recognition using masked priming ERP. *Frontiers in Psychology*, *3*, 333.

Taft, M., & Zhu, X. (1997). Submorphemic processing in reading Chinese. *Journal of Experimental Psychology: Learning Memory and Cognition*, *23*(3), 761–774.

Taft, M., Zhu, X., & Peng, D. (1999). Positional specificity of radicals in Chinese character recognition. *Journal of Memory and Language*, *40*(4), 498–519.

Tamaoka, K., & Yamada, H. (2000). The effects of stroke order and radicals on the knowledge of Japanese kanji orthography, phonology and semantics. *Psychologia*, *43*(3), 199–210.

Tan, L. H., Hoosain, R., & Peng, D. (1995). Role of early presemantic phonological code in Chinese character identification. *Journal of Experimental Psychology: Learning, Memory, and Cognition*, *21*(1), 43–54.

Tan, L. H., Liu, H. L., Perfetti, C. A., Spinks, J. A., Fox, P. T., & Gao, J. H. (2001). The neural system underlying Chinese logograph reading. *Neuroimage*, *13*(5), 836–846.

Tani, T. (2004). A case of alexia with agraphia of Kanji following left posterior inferior temporal lobe infarction (in Japanese). *Higher Brain Function Research*, *24*(4), 343–352.

Thesen, T., McDonald, C. R., Carlson, C., Doyle, W., Cash, S., Sherfey, J., … Devinsky, O. (2012). Sequential then interactive processing of letters and words in the left fusiform gyrus. *Nature Communications*, *3*, 1284.

Tsunoda, K., Yamane, Y., Nishizaki, M., & Tanifuji, M. (2001). Complex objects are represented in macaque inferotemporal cortex by the combination of feature columns. *Nature Neuroscience*, *4*(8), 832–838.

Ungerleider G., L. (1982). Two cortical visual systems. *Analysis of Visual Behavior*, 549–586.

Uno, A., Wydell, T. N., Haruhara, N., Kaneko, M., & Shinya, N. (2008). Relationship between reading/writing skills and cognitive abilities among Japanese primary-school children: normal readers versus poor readers (dyslexics). *Reading and Writing*, *22*(7), 755–789.

van der Mark, S., Bucher, K., Maurer, U., Schulz, E., Brem, S., Buckelmuller, J., … Brandeis, D. (2009). Children with dyslexia lack multiple specializations along the visual word-form (VWF) system. *Neuroimage*, *47*(4), 1940–1949.

van der Mark, S., Klaver, P., Bucher, K., Maurer, U., Schulz, E., Brem, S., … Brandeis, D. (2011). The left occipitotemporal system in reading: disruption of focal fMRI

connectivity to left inferior frontal and inferior parietal language areas in children with dyslexia. *Neuroimage*, *54*(3), 2426–2436.

Vinckier, F., Dehaene, S., Jobert, A., Dubus, J. P., Sigman, M., & Cohen, L. (2007). Hierarchical coding of letter strings in the ventral stream: Dissecting the inner organization of the visual word-form system. *Neuron*, *55*(1), 143–156.

Warrington, E. K., & Shallice, T. (1980). Word-form dyslexia. *Brain*, *103*(1), 99–112.

Wolpert, I. (1924). Die simultanagnosie — störung der gesamtauffassung. *Zeitschrift Für Die Gesamte Neurologie Und Psychiatrie*, *93*(1), 397–415.

Xiang, J.-Z., & Brown, M. W. (1998). Differential neuronal encoding of novelty, familiarity and recency in regions of the anterior temporal lobe. *Neuropharmacology*, *37*(4), 657–676.

Yeatman, J. D., Rauschecker, A. M., & Wandell, B. A. (2013). Anatomy of the visual word form area: adjacent cortical circuits and long-range white matter connections. *Brain and Language*, *125*(2), 146–155.

Zhang, H., Liu, J., & Zhang, Q. (2013). Neural correlates of the perception for novel objects. *PloS One*, *8*(4), e62979.

Zhou, L., Peng, G., Zheng, H.-Y., Su, I.-F., & Wang, W. S.-Y. Y. (2012). Sub-lexical phonological and semantic processing of semantic radicals: a primed naming study. *Reading and Writing*, *26*(6), 1–23.

Appendix A

Lists of stimuli for experiment 1

List of real *Kanji* characters

List of pseudo *Kanji* characters

List of artificial *Kanji* characters

Appendix B

Lists of stimuli for experiment 2

List of real objects

List of pseudo objects

List of artificial patterns

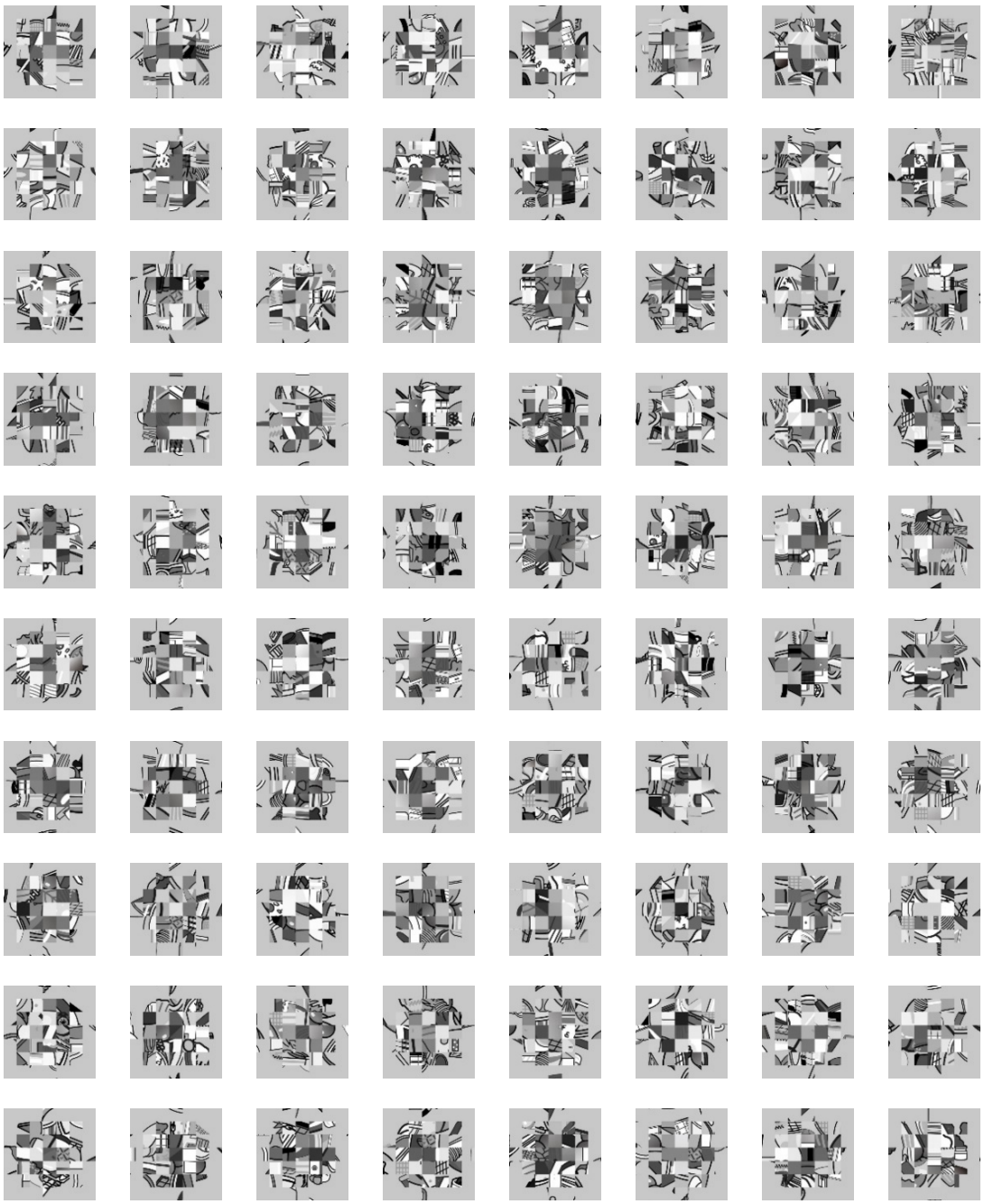

List of control stimuli